Journal of Vertebrate Paleontology e1781143 (18 pages)
© by the Society of Vertebrate Paleontology
DOI: 10.1080/02724634.2020.1781143

Check for updates

ARTICLE

AN ENIGMATIC NEODIAPSID REPTILE FROM THE MIDDLE TRIASSIC OF ENGLAND

IACOPO CAVICCHINI,† MARTA ZAHER, and MICHAEL J. BENTON *
School of Earth Sciences, University of Bristol, Bristol, BS8 1RJ, U.K., iacopo.cavicchini@gmail.com; m.zaher@bristol.ac.uk; mike.benton@bristol.ac.uk

ABSTRACT—The fossil record of early diapsids is sparse, specimens are uncommon and often incomplete, and phylogenetic relationships are hard to determine. A new taxon of early diapsid, *Feralisaurus corami* from the Middle Triassic of Devon, south-western England, is here named and described from an incomplete but mostly articulated skeleton, comprising skull, vertebrae, pectoral girdle, ribs, and the right forelimb. CT scanning and the resultant 3D model of the skeleton reveal anatomical details otherwise buried in the sandstone matrix. This new diapsid is characterized by a plesiomorphically high maxilla without a prominent nasal process, a quadrate with a lateral conch, a low jugal with small posterior process, conical teeth with pleurodont implantation, a high coronoid process, notochordal vertebrae, a long humerus with an entepicondylar foramen, rod-like clavicles, a 'T'-shaped interclavicle, and a ventrolateral process of the scapulocoracoid. Phylogenetic analyses, although showing generalized weak support, retrieved *Feralisaurus* within Neodiapsida or stem-group Lepidosauromorpha: its morphology supports the latter hypothesis. This specimen adds to our knowledge of the early diversification of Lepidosauromorpha and of English Middle Triassic terrestrial faunas.

http://zoobank.org/urn:lsid:zoobank.org:pub:15C79035-61C3-4F45-910F-FE5749AA15A0

SUPPLEMENTAL DATA—Supplemental materials are available for this article for free at www.tandfonline.com/UJVP

Citation for this article: Cavicchini, I., M. Zaher, and M. J. Benton. 2020. An enigmatic neodiapsid reptile from the Middle Triassic of England. Journal of Vertebrate Paleontology. DOI: 10.1080/02724634.2020.1781143.

INTRODUCTION

Lepidosauria is a clade comprising two subclades, Squamata (lizards and snakes) and Rhynchocephalia (sphenodontians), with more than 10,000 living species (www.reptile-database.org). However, in spite of their evolutionary success, the early history of Lepidosauria is unclear. Fossil specimens and phylogenomic analyses show that Squamata and Rhynchocephalia diverged by the Early Triassic (e.g., Evans, 2003; Evans and Jones, 2010; Jones et al., 2013). Whereas there are several well-described rhynchocephalian taxa from the Late Triassic, older materials of that clade, Triassic squamates and stem-group lepidosauromorphs, are few in number, usually incomplete, and their phylogenetic attribution is often problematic (Carroll, 1975; Evans, 1991; Waldman and Evans, 1994; Evans, 2003; Modesto and Reisz, 2003; Evans and Borsuk-Białynicka, 2009; Renesto and Bernardi, 2014; Schoch and Sues, 2018; Simões et al., 2018).

Currently the oldest recognized lepidosauromorph is *Paliguana* from the Lower Triassic of South Africa (Carroll, 1975). However, the worldwide record of such taxa is patchy and most come from Europe: Kuehneosauridae from North America, England and Poland, *Sophineta* from the Early Triassic of Poland, *Fraxinisaura* from the Middle Triassic of Germany, and *Coartaredens* from the Middle Triassic of England (Evans, 1991; Spencer and Storrs, 2002; Evans, 2009; Evans and Borsuk-Białynicka, 2009; Schoch and Sues, 2018). The Italian Middle Triassic *Megachirella* has had a checkered history, being described first as a lepidosauromorph (Renesto and Posenato, 2003), then as a dubious squamate (Renesto and Bernardi, 2014), and then as the oldest definite squamate (Simões et al., 2018). The first undisputed lepidosaurs are known from the Middle Triassic but are rhynchocephalians (Jones et al., 2013); crown-group Squamata have been found in strata no older than Early Jurassic (Evans, 1988; Evans et al., 2002), implying the existence of a substantial ghost lineage for Squamata. Relationships among these early diverging taxa are unresolved but should be determined if we are to understand the early evolution of extant lepidosaurs.

Middle Triassic strata in the U.K. have been known for more than a century as a source of vertebrate fossils (Spencer and Isaac, 1983; Benton, 1997; Coram et al., 2019), but so far they have yielded nothing more than fragmentary remains of possible lepidosauromorphs. Here we expand the record of Triassic lepidosauromorphs by describing and naming a new taxon from the Otter Sandstone of Devon and give an assessment of its phylogenetic position.

Institutional Abbreviation—BRSUG, University of Bristol, School of Earth Sciences, Bristol, U.K.

MATERIALS AND METHODS

Geological Setting and Preservational Context

The Otter Sandstone, exposed for ca. 10 km along the coast of Devon from Budleigh Salterton to Sidmouth, has long been known as a source of vertebrate fossils (Spencer and Isaac, 1983; Spencer and Storrs, 2002; Coram et al., 2019). Note that the term 'Otter Sandstone Formation' of former use has been dismissed; the outcrops in the south-western U.K. originally assigned to that unit are now part of the Helsby Sandstone Formation, a

*Corresponding author.
†Current address: Dipartimento di Scienze della Terra, Sapienza Università di Roma, Piazzale Aldo Moro 5, 00185 Roma, Italy

Color versions of one or more of the figures in the article can be found online at www.tandfonline.com/ujvp.

Published online 05 Oct 2020

thick sandstone-dominated unit that extends from Devon to Cumbria (Ambrose et al., 2014).

The Helsby Sandstone Formation achieves a maximum thickness of 210 m in Devon and is composed of reddish sandstones and subordinate conglomerates and mudstones; the depositional environment was a network of braided or meandering rivers, bringing water and life to an otherwise arid continental landscape (Ambrose et al., 2014; Coram et al., 2019). The origin of the rivers was located in modern-day France, and the waters flowed northward to the Irish Basin; outcrops of the Helsby Sandstone Formation track this ancient, huge river system, spanning from the south-west to the north of England. Fluvial systems developed at least twice in the U.K. during the Triassic, following intervals of tectonic stasis in an otherwise west-to-east directed extensional regime, as testified by the transgressive character of the overlying, Upper Triassic Mercia Mudstone Formation and Penarth Group (Newell, 2018). We use the informal term 'Otter Sandstone' here to indicate the red, Middle Triassic outcrops along the south-east Devon coast where our specimen was found.

Magnetostratigraphic studies of the Otter Sandstone indicate an Anisian age (Hounslow and McIntosh, 2003), confirmed by the present extinct rhynchosaur and amphibian taxa, thus correlating the Otter Sandstone with the Muschelkalk of the Germanic Basin and the Donguz Svita of European Russia (Benton, 1997; Hounslow and McIntosh, 2003).

The Otter Sandstone has yielded many fossils, including reptile, temnospondyl amphibian and fish fossils, as well as arthropods, plants, and trace fossils (Milner et al., 1990; Spencer and Isaac, 1983; Spencer and Storrs, 2002; Coram and Radley, 2015; Coram et al., 2019). Fossils here are most commonly disarticulated bones in coarse channel lag conglomerates, but rarer articulated or associated skeletons from channel bars are also known (Benton, 1997; Coram et al., 2019; Zaher et al., 2019). Along with the neopterygian fishes, fresh-water sharks, temnospondyl amphibians, rauisuchids, rhynchosaurs, and procolophonids, there is a previously described genus of lepidosauromorph, *Coartaredens* (Spencer and Storrs, 2002), although known from only a few bone fragments.

Specimen and Sampling

The new specimen, BRSUG 29950-12, was found by Robert Coram in October 2014, west-south-west of a beach access at Jacob's Ladder, Sidmouth (National Grid Reference SY 109865), just beneath Peak Hill, after a storm had cleared a foreshore exposure at the top of the Otter Sandstone (Fig. 1). The specimen was found in a 40-mm-thick bed of yellowish, heterogeneous sandstone with rhizoliths, mudstone pebbles, carbonate concretions, coprolites, and vertebrate remains. Levels above and below show similar heterogeneity, especially the overlying levels that present alternations of mudstones, heterolithic sandstones, and clay pebble conglomerates.

This specimen comprises the incomplete skeleton, exposed in dorsal view (Fig. 2A), of a small diapsid (Figs. 2B, C, 3). Bones include portions of the skull, cervical and dorsal vertebrae up to the 19th or 21st presacral, the pectoral girdle, the right forelimb, and fragments of ribs. Missing portions of the axial skeleton could be linked to recent or contemporary erosion, whereas the left forelimb seems to be truly absent from the specimen either because of peri-mortem or post-mortem damage. Robert Coram carried out some minimal physical preparation of the specimen after discovery. The specimen was mostly exposed as it is now, and preparation was minimal (largely because of the extreme delicacy of the specimen). It was gently washed, and a small number of incompletely exposed elements were manually exposed further under a binocular microscope. Because of the extremely soft and crumbly nature of the matrix and bones, they were consolidated where required with commercially available wood hardener.

The superficial portion of the specimen is compressed and was subjected to an anteriorly increasing degree of lateral stress: vertebrae pass from dorsal to almost dorsolateral exposure, but the skull has been affected the most, by both deformation and weathering. Bones buried in the matrix, even superficially, show only minor signs of deformation.

The retrieved bones are mostly articulated, hinting at little to no peri- or post-mortem transport; the animal was found in a channel lag deposit, associated with numerous other clasts representing sedimentary debris. The channel is part of a subaerially exposed channel bar, later inundated by the ever-moving channel system and overlain by a coarser heterogeneous channel lag deposit. This interpretation is confirmed by the presence of rhizoliths, desiccation cracks and footprints on the top surface (Coram et al., 2019), before the channel lag brought about a short-lived burst of energy, depositing the coarser sediments that entombed the animal.

3D Model Creation

BRSUG 29950-12 was CT scanned at the University of Bristol, U.K., on a Nikon X-Tek H 225 ST X-ray scanner in two sessions (anterior and posterior portions of the specimen), both at 225 kV and 29 μA from a rotating tungsten target, with 2.0 s exposure, 0x binning, 3 dB gain, and a 2.5 mm copper filter. Slice thickness is 48.45 μm, for a total number of slices equal to 2735. Each scan captured 3141 projections, with four frames averaged per projection. The two sets of reconstructed scan data were subsequently combined in VGStudio (version 3; www.volumegraphics.com). A three-dimensional model was created from the CT data using the segmentation tools in the software program Avizo (v. 9.1.1 Lite, Visualization Science Group; www.fei.com/software/amira-avizo). The combined use of CT scans and a segmentation tool makes it possible to search inside the matrix for skeletal material otherwise impossible to analyze; this was the case also for BRSUG 29950-12. Scans and 3D models can be found online at Dryad (https://datadryad.org/stash/share/woYwvIyn17PLCmgXNtut0S94-ZzPysxHDFxYFtYC6HE).

Data collected during the CT scanning process is displayed by the Avizo software as grayscale images, in which white and black represent, respectively, higher and lower densities, indirectly measured from the X-ray intensity (Abel et al., 2012). Skeletal material ideally has a consistently different density than rock matrix and the software is equipped with automatic and semi-automatic picking tools, which rely on this principle, to speed up the segmentation process. In this case, as well as in previous work on fossils from the Otter Sandstone (Zaher et al., 2019), the process had to be carried out manually: the Otter Sandstone is highly heterogeneous, comprising sand grains together with high-density clasts such as carbonate crystals and reworked fragments of rhizoliths.

This heterogeneity proved to be problematic in areas where high-density clasts clustered on and around the bones, making it difficult to separate the skeletal material from the matrix. Damaged portions of bones, with diminished density and dimensions, were another source of uncertainty during segmentation. However, most of the bones could be highlighted with confidence, except for some concerns about the ends of forelimb bones. It was a completely different matter, unfortunately, for the skull bones, most of which are compressed, disarticulated and damaged beyond recognition. The fragments were singled out as much as possible during the segmentation process with particular care, then they were identified or interpreted based entirely on the resulting 3D models.

Phylogenetic Analyses

Establishing the phylogenetic position of early lepidosauromorphs is difficult because of a general absence of preservable apomorphies, but also because there are multiple available

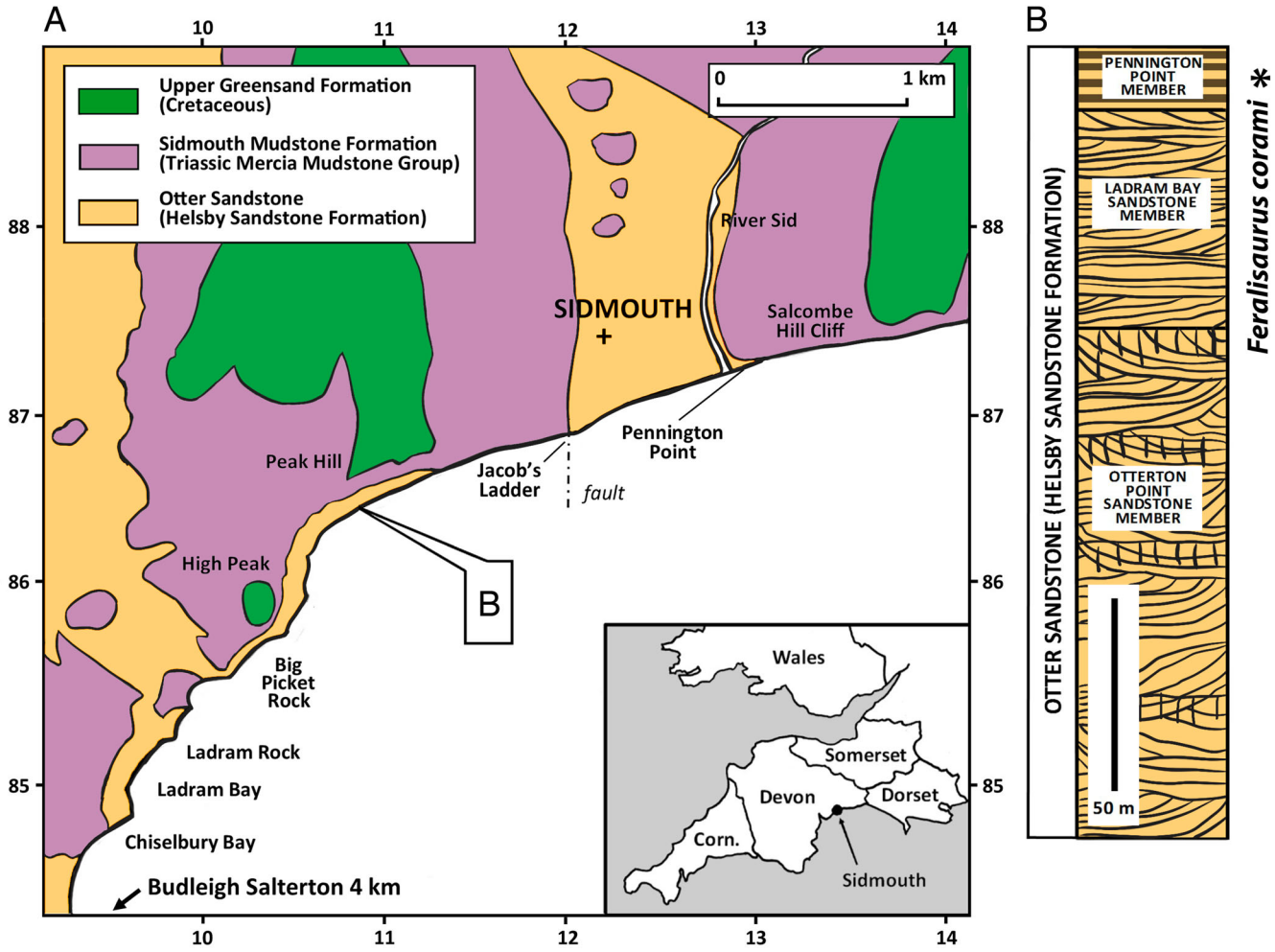

FIGURE 1. **A**, geological sketch map of the coast around Sidmouth, Devon and **B**, Otter Sandstone succession (adapted from Gallois, 2013), with asterisk showing the find location of BRSUG 29950-12. The numbers around the edge of the map correspond to the Ordnance Survey national grid reference system and are at 1 km intervals. **Abbreviation**: **Corn.**, Cornwall. Map courtesy of Rob Coram.

cladistic character matrices that cover very different arrays of taxa (e.g., Jones et al., 2013; Ezcurra et al., 2014; Schoch and Sues, 2018; Simões et al., 2018, 2020; Scheyer et al., 2020). In order to establish the phylogenetic position of BRSUG 29950-12, we carried out two sets of analyses, using PAUP 4.0 (Swofford, 2015) and TNT (Goloboff et al., 2008). Datasets were taken from Jones et al. (2013), from Schoch and Sues' (2018) version of the Ezcurra et al. (2014) matrix, from Simões et al. (2020) and from Scheyer et al. (2020), and run separately using both programs (codings for the specimen can be found in the Supplemental Data 1).

PAUP analyses were carried out using heuristic searches with a high number of repetitions and maximum number of trees, in order to get a stable and repeatable most parsimonious result. The analysis of the Schoch and Sues (2018) matrix used a heuristic search (over 2,000 maximum trees, random addition sequence with 40 replicates, TBR branch-swapping algorithm holding 1 tree after each repetition); repeating the same search on the resulting most parsimonious trees did not improve the topology. The analysis using the Jones et al. (2013) matrix was conducted with an identical approach in terms of software parameters and operations, except for the random addition sequence, which was set at 10 replicates.

TNT analyses were run as parsimony and new technology (NT) searches. In the parsimony search, space was set for 10,000 trees in memory, and 10 random addition sequences were carried out with tree bisection reconnection (TBR) branch-swapping, and bootstraps and Bremer supports calculated from 1,000 replicates for both strict and majority rule trees. In the NT search, the ratchet, drifting, sectorial searches, and tree-fusing methods were performed, majority rule and consensus trees calculated, and bootstraps and Bremer supports calculated from 1,000 replicates.

SYSTEMATIC PALEONTOLOGY

DIAPSIDA Osborn, 1903
NEODIAPSIDA Benton, 1985
LEPIDOSAUROMORPHA Gauthier, 1984
FERALISAURUS, gen. nov.

Type and Only Species—*Feralisaurus corami*.
Etymology—Latin adjective 'feralis,' meaning wild, and refers to the presumed predatory habits of *Feralisaurus*.
Diagnosis—As for species.

FERALISAURUS CORAMI, sp. nov.

Holotype—BRSUG 29950-12, a partial skeleton of well-articulated or associated bones, including skull, mandible, 19–21 presacrals, ribs fragments, pectoral girdle, and the right forelimb.

Etymology—To honor Robert Coram, discoverer of the holotype.

Dimensions—Mandible ramus length = 28.39 mm; mandible width (coronoid, estimate) = 12.68 mm; skull length (estimate) = 33.94 mm; estimated presacral body length = 120.3–132.95 mm; humerus length = 23.28 mm; ulna length = 14.74 mm; radius length = 14.03 mm; interclavicle width = 13.87 mm; interclavicle length (incomplete) = 6.06 mm.

Horizon and Locality—Pennington Point Member, Helsby Sandstone Formation (former Otter Sandstone Formation), Sherwood Sandstone Group, Anisian, Middle Triassic. Foreshore below Peak Hill, Sidmouth, East Devon, England (National Grid Reference: SY 109865).

Diagnosis—A small neodiapsid characterized by the following: maxilla high but without a prominent nasal process; jugal with a low dorsal process and small rounded posterior process; teeth conical with pleurodont implantation; mandible with high coronoid process and medium-length retroarticular process; modest transverse processes on vertebrae; rod-like clavicles; robust interclavicle without an anterior process; broad unfenestrated coracoids; ventrolateral process of scapulocoracoids; single-headed ribs.

DESCRIPTION

The description of BRSUG 29950-12 is mostly based upon the 3D model (Figs. 2, 3), to account for the wealth of details that emerged only after the segmentation process, although the skeletal material is concentrated on the block's surface or immediately below.

Skull and Mandible

General Comments—The skull bones are generally poorly preserved. Compression and a considerable amount of lateral stress have acted on the area (the most notable evidence is the fact that the right maxilla lies flat, with its internal side upwards), obliterating finer details and disarticulating the skull; the upper parts of the skull had been exposed on the surface of the slab and subjected to erosion. It is possible to determine the length and width of the skull, but its height is uncertain. The length and width of the mandible, 28.4 mm and 12.7 mm, respectively, suggest an estimated skull length of 33.9 mm.

In the snout region, the right maxilla is identified with confidence, and is described in more detail below. Among other elements in this area, a bone fragment is interpreted as an incomplete premaxilla (Figs. 2B, 3A) with a 2.25 mm high, gracile and gently curved portion of the nasal process preserved, but it reveals no further data about teeth, articulations or size and shape of the nares. An additional bone fragment, 3.3 mm long, embedded in the matrix just dorsally of the maxilla, is interpreted as an incomplete right prefrontal because of its dorsoventral curvature (Fig. 2B, C). However, there are no clear CT data about palatal bones, the possible presence of a lacrimal or its extent, or the size and shape of the orbits.

At the end of the suborbital ramus of the maxilla, a flattened, triangular element with rounded edges and a facet visible on its anterior process is interpreted as the right jugal (Figs. 2C, 3A, 4C, D); it shows a low dorsal process and small rounded posterior process. The length of the maxilla and the jugal together (18.7 mm) is compatible with the length of the mandible between the symphysis and the highest point of the coronoid process (18.6 mm), which confirms the interpretation. It has a rounded, modest posterior process, whereas the indent of the ventral margin looks just damaged and the postorbital process is almost certainly incomplete; the overall morphology is comparable to that of other early lepidosauromorphs, and the posterior process in particular is similar to that of *Fraxinisaura* (Schoch and Sues, 2018), different from the sharp process found in *Megachirella* or the spur of *Marmoretta* or *Sophineta* (Evans, 1991; Evans and Borsuk-Białynicka, 2009; Renesto and Bernardi, 2014). Fragments of the postorbital region are also present in the area: in particular, a 3.5 mm long fragment of bone almost on the surface of the block, with the medially directed end partially branched is interpreted as an incomplete right postorbital (Figs. 2B, 4H).

The posterior and medial areas of the skull present some flat fragments of the parietals, frontals, and right squamosal, on the surface of the block (Figs. 2, 4A); below them, some loosely associated material could be remnants of the braincase, judging by their shape and association. Above the adductor fossa of the mandible, embedded in the matrix, a skeletal element is interpreted as an incomplete right quadrate or quadratojugal, from its position and the peculiar conch it displays in anteroposterior view (Figs. 2C, 4E–G).

Maxilla—The right maxilla lies completely inside the matrix, directly above the mandible with its medial side up, and looks reasonably complete (Figs. 2C, 3A, 4A, B). The left maxilla is absent. The maxilla is 14.6 mm long, slender, elongated and plesiomorphically high, but lacks a prominent facial process, much unlike the stout process found in *Sophineta*, or the low maxilla and weak facial processes of *Marmoretta* and *Fraxinisaura* (Evans, 1991; Waldman and Evans, 1994; Evans and Borsuk-Białynicka, 2009; Schoch and Sues, 2018); the morphology resembles the maxilla in less derived forms, like *Paliguana* (Carroll, 1975) or *Youngina* (Gow, 1975). The maximum height of the bone (2.4 mm) is achieved at a quarter of its length, above the 5th and 6th teeth, and then it steadily decreases posteriorly. The suborbital ramus is posteriorly elongated enough to presume its involvement in the anteroventral margin of the orbit, whereas the premaxillary ramus area is not quite as clear and the anterior-most tip may be missing. The ventral margin is straight for roughly two-thirds of the total length and then it curves gently dorsally at an angle equal to the dorsal side's slope. The maxilla bore 25 teeth in life, as indicated by teeth and tooth positions, but only 13 teeth are preserved in situ. They are small, conical and roughly circular in cross section, with a pointed tip; the maxilla also presents a strong lingual shelf developed above the teeth. The shape of the teeth is roughly constant, but height and diameter decrease towards the posterior end of the bone. Anterior teeth tend to be curved distally but this may be an artifact of compression. The resolution of the scan does not reveal much detail of the tooth surface.

Hyoid Apparatus—The ossified first branchial horns (or ceratobranchials) are partially preserved in the matrix below the mandible, not in their life position (Figs. 2, 3). They are small and elongated, with a slightly dorsoventrally flattened section, and curved medially and ventrally. The rest of the apparatus was not found, possibly because it was cartilaginous.

Mandible—The right ramus of the mandible is preserved entire, with most of the dentition, although not articulated with the skull, whereas the posterior half of the left ramus was exposed and probably eroded away, leaving only the anterior portion of dentary, splenial, and a few teeth (Fig. 4I, J). The symphysis area is also damaged, so now the two rami are slightly dislocated from each other. Apart from this, the mandible looks as if it has suffered only minor deformation and a slight distal tilt (20–30° around the long axis of the bone) for the right ramus; thus, the description is based on the 3D model and, in places, on CT scan images. Sutures are not clear enough from the CT data to be identified for the full length of the mandible; the anterior-most portion of the dentary-splenial contact was the only exception, allowing us to determine unequivocally the presence of a splenial bone.

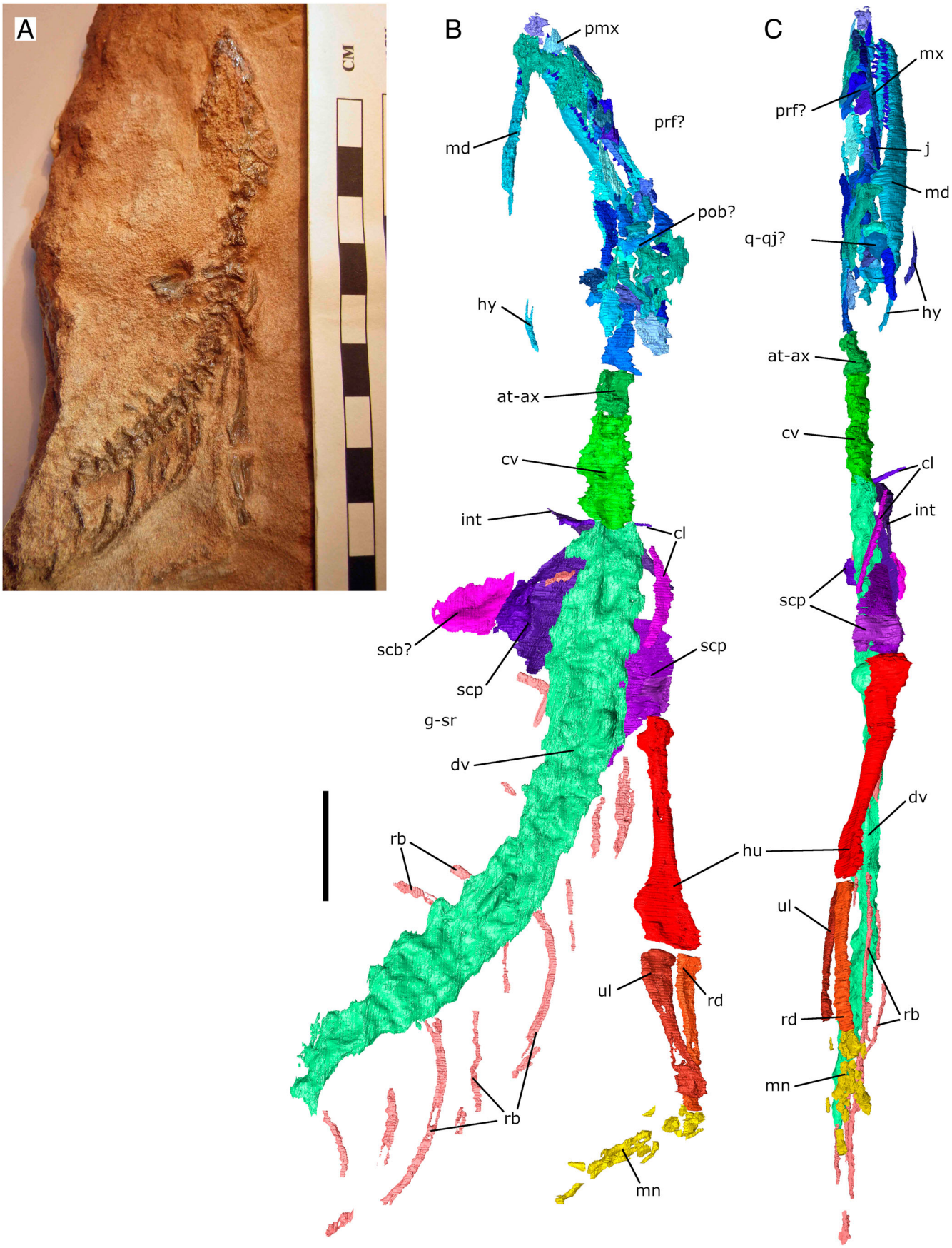

FIGURE 2. *Feralisaurus corami*, gen. et sp. nov., specimen and skeletal restoration. **A**, BRSUG 29950-12, holotype, specimen in dorsal view in its sandstone matrix, and following some minimal physical preparation. Image courtesy of Rob Coram. **B**, **C**, BRSUG 29950-12, holotype, 3D digital representation in **B**, dorsal and **C**, right lateral views. **Abbreviations**: **at-ax**, atlas and axis complex; **cl**, clavicle; **cv**, cervical vertebrae; **dv**, dorsal vertebrae; **g-sr**, gastralia/sternal ribs; **hy**, hyoid; **hu**, humerus; **incl**, interclavicle; **j**, jugal; **md**, mandible; **mn**, manus; **mx**, maxilla; **pmx**, premaxilla; **pob?**, postorbital; **prf?**, prefrontal; **q-qj?**, quadrate/quadratojugal; **rb**, ribs; **rd**, radius; **scb**?, scapular blade; **scp**, scapulocoracoid; **ul**, ulna. Scale bar equals 1 cm (**B**, **C**).

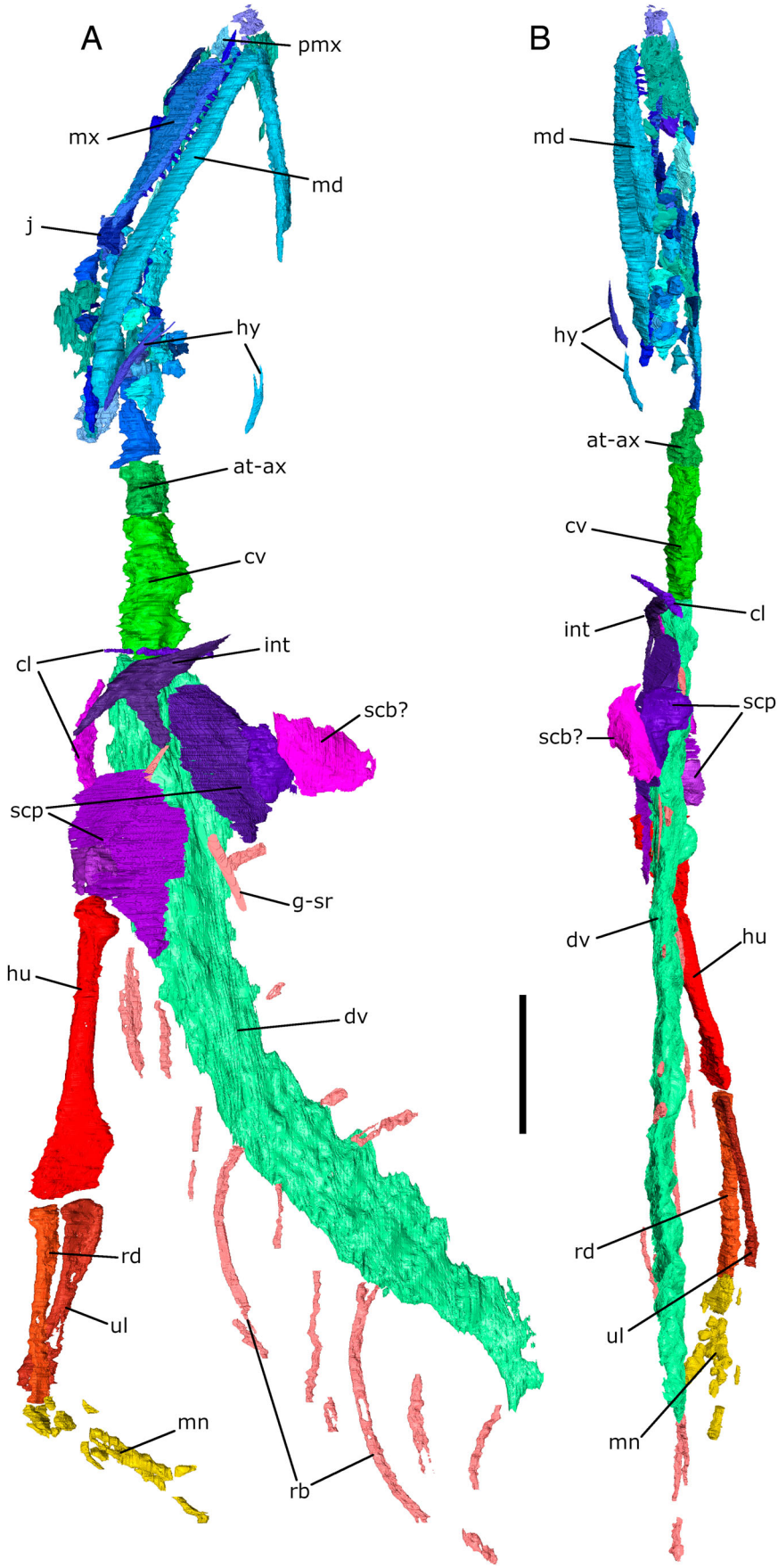

FIGURE 3. *Feralisaurus corami*, gen. et sp. nov. holotype specimen BRSUG 29950-12, 3D digital representation in **A**, ventral and **B**, left lateral views. **Abbreviations**: **at-ax**, atlas and axis complex; **cl**, clavicle; **cv**, cervical vertebrae; **dv**, dorsal vertebrae; **g-sr**, gastralia/sternal ribs; **hy**, hyoid; **hu**, humerus; **incl**, interclavicle; **j**, jugal; **md**, mandible; **mn**, manus; **mx**, maxilla; **pmx**, premaxilla; **rb**, ribs; **rd**, radius; **scb?**, scapular blade; **scp**, scapulocoracoid; **ul**, ulna. Scale bar equals 1 cm.

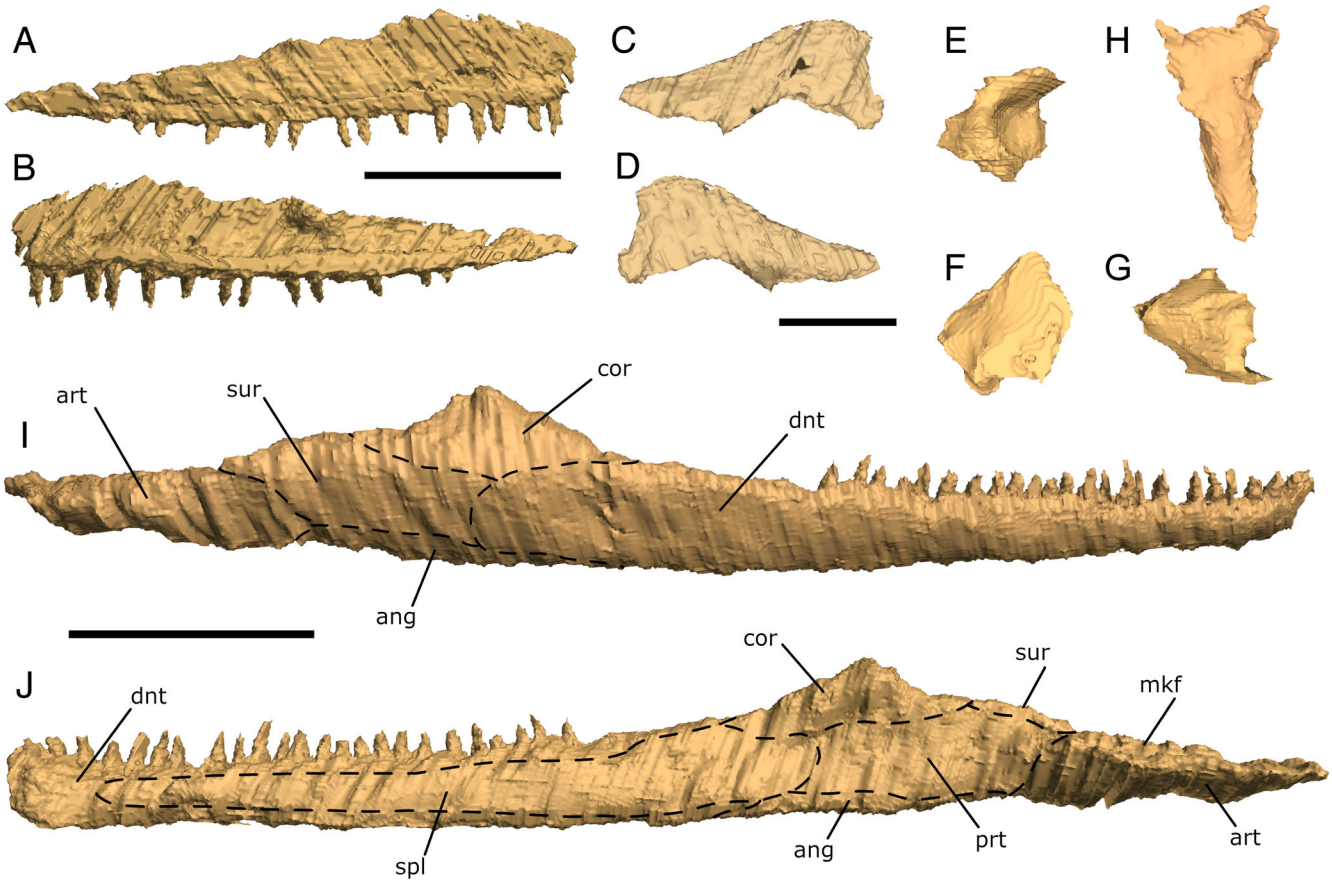

FIGURE 4. *Feralisaurus corami*, gen. et sp. nov., BRSUG 29950-12, holotype, 3D digital representation of right-hand skull elements. **A**, **B**, maxilla in **A**, labial and **B**, lingual views. **C**, **D**, right jugal in **C**, internal and **D**, external views. **E**–**G**, right quadrate/quadratojugal in **E**, ventral, **F**, external, and **G**, dorsal views. **H**, right postorbital in dorsal view. **I**, **J**, right mandibular ramus in **I**, labial and **J**, lingual views. **Abbreviations**: **ang**, angular; **art**, articular; **cor**, coronoid; **dnt**, dentary; **mkf**, Meckelian fossa; **prt**, prearticular; **spl**, splenial; **sur**, surangular. Scale bars equal 5 mm (**A**, **B**), 2 mm (**C**–**H**), and 5 mm (**I**, **J**).

The mandible is long, relatively slender, and laterally compressed. It is gently convex on both internal and external sides, except just below the coronoid process, where there is a slight concavity on the medial side. The two rami are roughly in life position, separated by a 40° angle. The dorsal and ventral margins of the rami are not parallel: the smooth, rounded ventral margin maintains a constant, gently curved outline, unlike the height variations seen in the mandibular ventral side of *Fraxinisaura* (Schoch and Sues, 2018); the dorsal margin rises slowly until about two-thirds of the total length to form the coronoid process, which is considerably higher than the tooth level. The two margins have similar inclination and steepness. This process is higher and stouter in *Feralisaurus* if compared with other lepidosauromorph coronoid processes described or reconstructed in the literature (Carroll, 1975; Evans, 1991; Renesto and Bernardi, 2014; Schoch and Sues, 2018). Behind the coronoid process, the dorsal margin slopes down posteriorly and flares laterally to both sides to form the dorsally concave adductor fossa and, further posteriorly, the articular surface. In dorsal view, the mandibular ramus is straight from the symphysis to the coronoid process, then it bends slightly proximolaterally. The post-coronoid portion is the widest part of the mandible, its surface slightly more dorsal than the level of the tooth row. All surfaces of the mandible bear no visible ridges or ornamentation. The articular surface is short (Fig. 4J), indicating orthal rather than propalinal motion (Romer, 1956).

Splenials are partially visible in the CT data, extending on the lingual and ventral side of the mandibular rami from a point close to the dentary's tip (but apparently not contributing to the symphysis), with a progressively larger section at the expense of the dentary. The maximum dimension is achieved at about half the length of the mandible, then decreases steadily backwards; its posterior termination is not visible.

The section of the dentary maintains roughly constant shape and dimensions for about a third of the mandible's length, then it narrows to a thin blade, stretching posteriorly on the labial side for at least half its length. The labial wall is dorsoventrally taller than the lingual wall, but the difference can be insignificant in places.

The post-coronoid morphology of the mandible is clear, though sutures were not visible in this area (Fig. 4I, J). The adductor fossa is moderately deep and roughly ellipsoidal in dorsal view, its flanks describing a fairly open 'V.' The Meckelian canal extending from the fossa is easily observable and can be followed for the whole length of the mandible. The articular surface was not easy to highlight because of high matrix heterogeneity in the area, but it appears to retain some of the adductor fossa's dorsally directed concavity; the retroarticular process is clear and modestly elongated if compared with those of kuehneosaurids or *Megachirella* (Renesto and Posenato, 2003; Evans, 2009; Evans and Jones, 2010). Together, the post-coronoid portion of the mandible accounts for roughly one quarter of the total length.

Teeth—The right, intact, dentary bore 26 teeth in life, 23 of which are preserved in the specimen (Fig. 4I, J), whereas the incomplete left dentary has only six (Figs. 2, 3). The teeth are very small, conical, and with a sharp tip, although at this resolution it is impossible to see any ornamentation of the tooth surface. The teeth are sometimes posteriorly recurved and generally lie in the medial plane of the mandible, although the first three teeth on the anterior margin of the dentary extend slightly distally. The anterior teeth generally have wider sections and are longer, whereas tooth morphology remains constant in the rest of the dentary. Tooth wear is difficult to assess: some tips are missing, but this could reflect post-mortem damage. The symphysis area is especially problematic, with bone fragments confusing the actual morphology. Teeth, however, are evident and they appear to be slightly longer than the other teeth, and they adopt a procumbent orientation, extending at 45° forward and laterally.

Tooth implantation is pleurodont, as can be seen clearly in digital renderings (Fig. 5A) and in individual CT images (Fig. 5B); in other words, the teeth sit in close contact on a shelf along the inside of the dentary and the maxilla which has a higher lip on the labial (lateral) side, and no lingual (medial) lip. The teeth are closely spaced, so much so that at this scan resolution they sometimes appear to be in close contact (Fig. 5B), and there is no sign of individual sockets for any of the teeth. The groove narrows posteriorly, as the teeth stand more vertically on the crest of the mandible (Fig. 5A).

Postcranial Skeleton

General Comments—Postcranial bones include the vertebral column up to the 19th–21st presacral, two almost complete ribs and a number of smaller fragments, the pectoral girdle and the right forelimb along with bones of the carpal region.

Vertebrae—The vertebral column is visible on the block's surface (Figs. 2, 3) and comprises 19–21 presacrals, lacking any sacrals or caudals, but is in a poor state of preservation. Compression and lateral stress have heavily deformed all the vertebrae, now flattened and pushed against each other. The vertebrae are more tilted towards the skull, being almost in dorsolateral view if seen from above; the last presacrals look only compressed on the specimen's surface.

Most of the details of zygapophyses and neural spines are lost to deformation and erosion (Figs. 2, 3). On the other hand, in some locations it is possible to observe the centra in section and to identify zygapophyses, but it was impossible to properly locate the suture between neural arches and centra and the space between the pre- and postzygapophyses of adjacent vertebrae. For these reasons and because of the heterogeneous matrix, vertebrae were not segmented separately during processing of the CT images.

Preservation quality decreases anteriorly throughout the vertebral column to a degree where it is difficult to interpret features of the cervical vertebrae or to give their exact number (either five or six); however, it was possible to separate the atlas and axis complex from the rest of the cervical vertebrae (Figs. 2, 3). The neck overall is 14.5 mm long, making roughly one fifth of the preserved vertebral column length; calculations of average lengths show that dorsals are almost twice as long as cervicals.

Dorsal vertebrae have a roughly rectangular outline in dorsal view and are wider than long, although this is probably due to deformation. The only dorsal vertebra in which a centrum can be identified with confidence is notochordal, but we can note only general flaring of the centrum at both anterior and posterior ends and the presence of one or two ventral keels. There are no

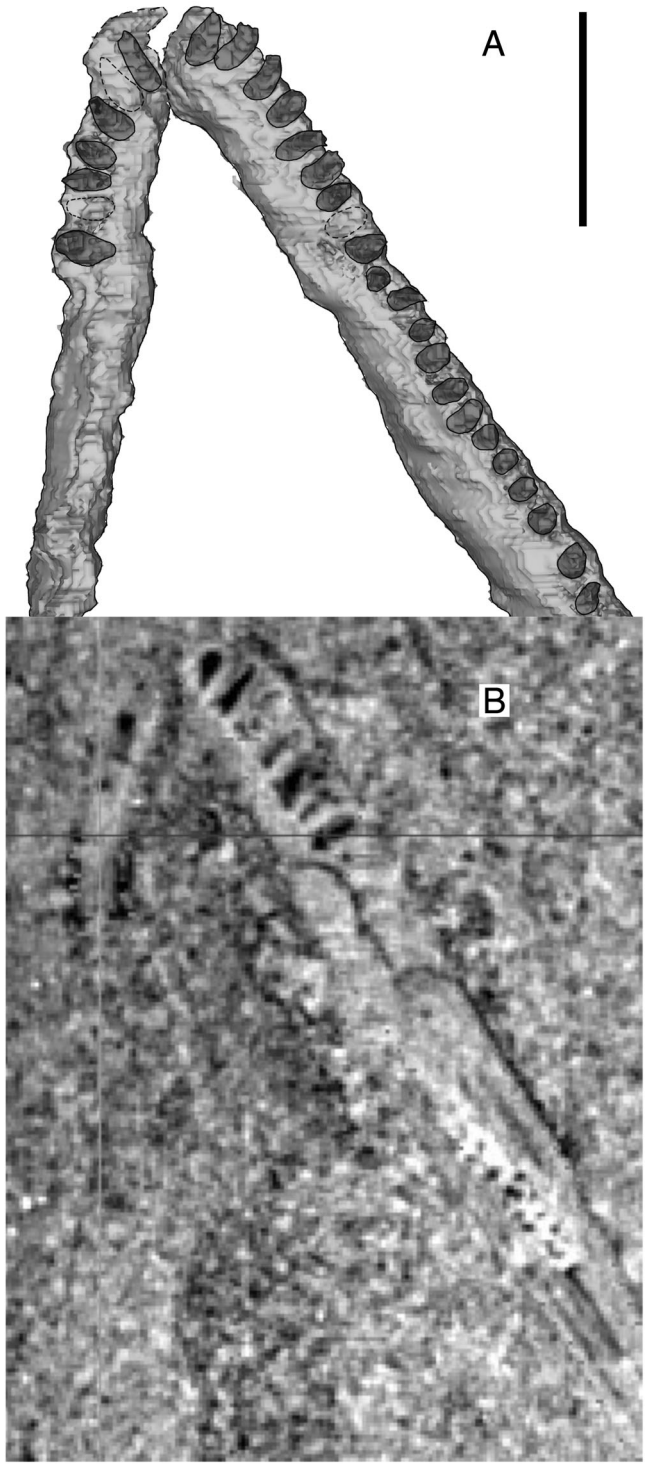

FIGURE 5. *Feralisaurus corami*, gen. et sp. nov., BRSUG 29950-12, holotype, 3D digital representation and CT scan of pleurodont tooth implantation. **A**, raw 3D model of the mandible (light gray), damaged on the left-hand side, showing numerous closely-spaced teeth (dark gray) sitting along a shelf that is lower lingually and higher labially. **B**, individual X-ray CT image showing close-packed anterior teeth of the mandible; the black represents open pulp cavities and the white on either side is dentine; there is no intervening bone between individual teeth. Scale bar equals 2.5 mm.

visible intercentra in the CT data, but they could be obscured by the heterogeneous matrix or by the deformation. Zygapophyses are slim and elongated, with a notable anterolateral or posterolateral extension; their articular surfaces are modestly flared, ovoid-shaped, and oriented roughly laterodorsally for prezygapophyses and lateroventrally for postzygapophyses.

Transverse processes are present on dorsal vertebrae, unlike *Sophineta*, in which they are lacking (Evans and Borsuk-Białynicka, 2009); they project to a modest extent distally or gently posterolaterally on the left side, whereas they are decidedly posterolaterally directed on the right side. The left side is probably the best because the transverse processes are less affected by deformation (Figs. 2B, 3A).

Ribs—Several dorsal ribs are exposed on the surface (Figs. 2, 3); no cervical ribs could be found during the segmentation process, but this does not rule out their presence. The left side has five heavily damaged ribs, each preserved only as a small fragment of the proximal end; the right side has two ribs in good preservation, although still incomplete, plus 12 smaller fragments. Almost all ribs are exposed on the specimen's surface, making each of them compressed to various degrees and obliterating their original curvature. Only rib numbers 5, 8, and 10 on the right side appear curved in an equivalent manner (the third quarter of the length of rib 5 was digitally reconstructed). Rib 1 on the right side is partially covered by matrix and by rib 2, which allowed a good degree of preservation of its slim, roughly circular cross section.

The proximal rib heads can be observed only in ribs 5 and 8 on the right side (Figs. 2B, 3A). Although expanded, the head of rib 5 appears holocephalous, whereas the proximal end of rib 8 could just be broken and torn, giving the impression of being two-headed.

Rib 8 is 18.5 mm long, the longest preserved rib fragment, and is attached to the 12th–13th dorsal vertebra (making it the 17th–18th presacral); this hints either at a very long and wide ribcage or at a very sharp reduction in the size of ribs after the 17th–18th presacral, considering an average presacral number between 23 and 26 (Romer, 1956).

Ventrally to the vertebral column, in the pectoral region, two very flattened bone fragments are tentatively interpreted as gastralia or, alternatively, as sternal ribs, due to their plate-like morphology (Figs. 2B, 3A).

Pectoral Girdle

General Comments—The bones of the shoulder girdle are all present in the specimen, in various degrees of preservation. Scapular blades are absent, probably eroded away, whereas the coracoids and the median process of the interclavicle are incomplete.

Clavicles—Both clavicles have suffered some degree of deformation, with the right one being dorsoventrally strongly compressed (Figs. 2, 3) and resulting in a flat, crescent-shaped bone exposed on the surface. The left clavicle is embedded in the matrix near the interclavicle (Figs. 2, 3) and is interpreted to more closely resemble the original shape (but not the length), although broken at around two-thirds of the length. The bone is rod-like, very slightly arched dorsoventrally, almost oval in section and with a pointed proximal end.

Interclavicle—This bone is robust and 'T'-shaped, with the posteriorly curved lateral processes showing a triangular-shaped cross section and tapering posterolaterally, describing a ventrally convex, dorsally concave shape with a small dorsoventrally oriented anterior cuspid (Fig. 6A–C). A small webbing of bone can be seen between the posterior and each of the lateral processes, more evident for the left process. The left process is modestly compressed and shows an indentation towards the tip, whereas the right process shows less signs of deformation. The posterior process is incomplete, dorsally flat and its transversal section is wider anteriorly, thus displaying a roughly triangular anteroposterior section; its dorsoventral section is wider than that of the lateral processes. The interclavicle is in contact with both clavicles, but they are dislocated from their life positions and there are no traces of clavicular facets. The absence of an anterior process in *Feralisaurus* is a morphology similar to that of other species usually considered basal, like *Saurosternon* (Carroll, 1975); other coeval species, like *Fraxinisaura*, possess a notable anterior process (Schoch and Sues, 2018).

Scapulocoracoids—Both scapulae are preserved, but the scapular blades are absent, possibly from erosion, since they would have been located above what is now the surface of the block (Figs. 2, 3). No sutures between scapulae and coracoids were identified during segmentation, possibly because the bones were partially fused in life. The base of the scapular blade presents a similar morphology in both bones, being a slim, anteriorly elongated oval in horizontal section; no glenoid fossae are preserved.

The coracoids differ in size and shape, possibly as a result of lateral deformation and compression; the left one looks less deformed and is therefore selected for description (Fig. 6D–G). It is a wide blade-like bone, with a curvature that goes from ventrally to dorsally concave; the right coracoid has a more pronounced dorsal concavity in its anterior portion, but this could be a result of lateral stress. The proximal margins of both bones look irregular, possibly from the presence of cartilage, and no evidence of foramina or fenestrae on the surface of either coracoid emerged from the CT data.

The left scapulocoracoid, considered as a whole, is more elongate posteriorly, but its glenoid area is probably incomplete: taking the position of the scapular blade as a reference, the right scapulocoracoid is less elongated posteriorly, but it is thicker in the vicinity of the head of the humerus. Further, each scapulocoracoid has a peculiar ventrolateral low but thick process, more evident on the left bone (Fig. 6E–G), around 3.5 mm long in the left scapulocoracoid and projecting distally between 1.2 and 1.5 mm; the process is placed anteriorly and ventrally with respect to the glenoid fossae so it looks as if it is not part of the humerus proximal articulation with the scapulocoracoid.

Unidentified—In lateral contact with the left scapulocoracoid, exposed on the specimen's surface, there is a quite large bone ('scb?' in Figs. 2, 3). It has a strong anterodorsally open concavity and, just behind it, a low, posteriorly directed process. Although this process resembles those on the right humerus, the presence of a complete coating of cortical bone in anteroposterior section and its peculiar curvature suggest it is a part of the left scapulocoracoid, broken off and displaced. The best fit for this fragment is as the scapular blade, broken and fallen off. In this case the process would represent the supraglenoid buttress.

Forelimb

General Comments—The only appendage preserved is the right forelimb, with humerus, ulna, and radius, which is in place and remarkably complete except for compression. It was possible to segment the bones with confidence. Some bones of the carpal region were also visible in the CT scan, embedded in the matrix and disarticulated.

Humerus—The humerus is exposed lying on its ventral side (Fig. 7A–D); it is cracked in several places and is possibly missing portions of the proximal articular surface and of the supracondylar process. There is a twist of about 90° between the proximal and distal articular ends. The proximal end is moderately expanded compared to the shaft and roughly triangular in section; the deltopectoral crest is readily recognizable as an

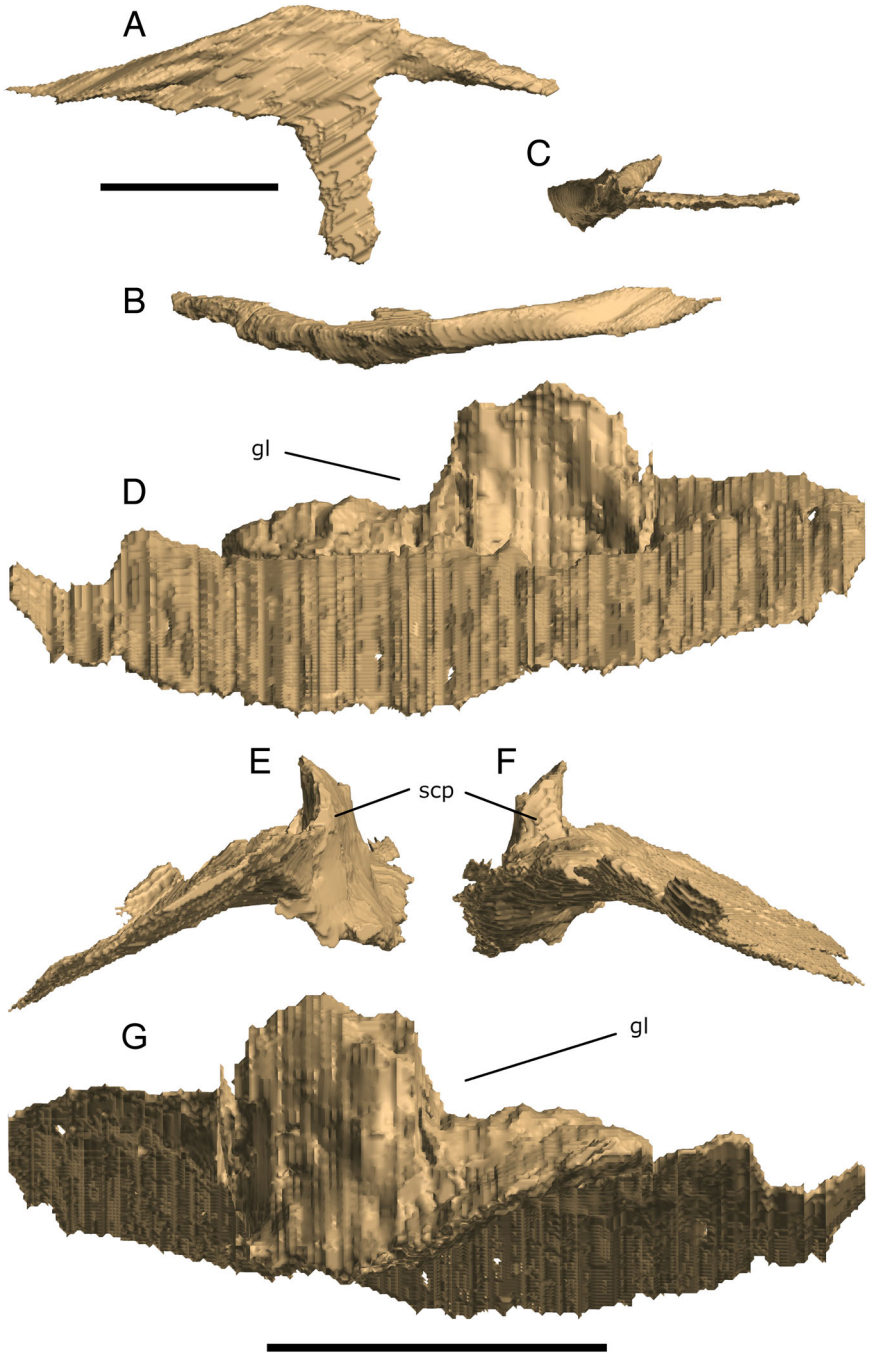

FIGURE 6. *Feralisaurus corami*, gen. et sp. nov., BRSUG 29950-12, holotype, 3D digital representation of shoulder girdle elements. **A**–**C**, interclavicle in **A**, dorsal, **B**, anterior and **C**, lateral views. **D**–**G**, left scapulocoracoid in **D**, right lateral, **E**, anterior, **F**, posterior, and **G**, left lateral views. **Abbreviations**: **gl**, glenoid (indication of where it is hypothesized to be); **scp**, scapular blade root. Scale bars equal 5 mm.

expansion that projects in a dorsolateral direction. The remaining morphology of the proximal articular surface is damaged and difficult to describe.

The shaft is long and preserved in its original shape for most of its length, at times breaking rather than deforming. The distal end of the bone is rather slim, flat, and wider than the proximal end, possibly partly because of deformation, and a portion of the ectepicondyle is probably missing. The supracondylar process and entepicondyle are slightly ridged with a flat surface between them, broken only ventrally by the capitulum tuberosity. There is a visible indentation on the ventral side of the entepicondylar process, which could be a remnant of the entepicondylar foramen, perhaps not completely open in life since the dorsal side bears no signs of it. Presence or absence of an ectepicondylar foramen cannot be confirmed. The distal articular surface is slim, and the trochlear surface is slightly curved.

Radius—The radius is slightly flattened dorsoventrally, although it twists anteriorly towards the distal end, which is moderately expanded and smaller than the proximal end (Fig. 7E, F). A shallow medial groove can be followed on the dorsal side of the bone, from just below the proximal epiphysis to about one third of the total length. The articular ends are flattened and present little detail at this scale.

Ulna—The ulna has a very damaged and possibly partially eroded distal end and the bone as a whole is flattened and twisted anterodorsally, possibly as a consequence of deformation

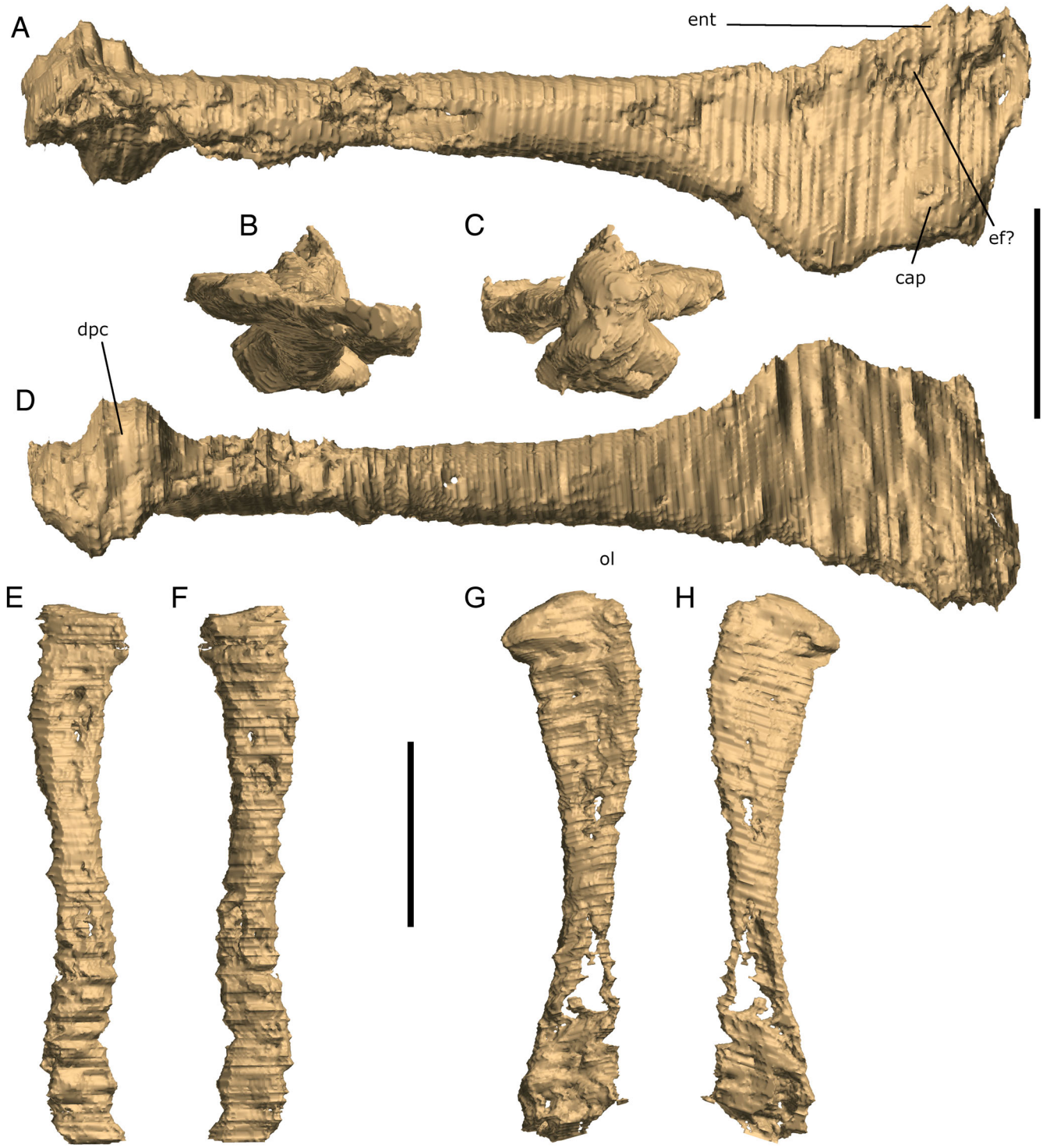

FIGURE 7. *Feralisaurus corami*, gen. et sp. nov., BRSUG 29950-12, holotype, 3D digital representation of right forelimb elements. **A**–**D**, humerus in **A**, dorsal, **B**, distal, **C**, proximal, and **D**, ventral views. **E**, **F**, radius in **E**, ventral and **F**, dorsal views. **G**, **H**, ulna in **G**, dorsal and **H**, ventral views. **Abbreviations**: **cap**, capitulum; **dpc**, deltopectoral crest; **ef?**, entepicondylar foramen; **ent**, entepicondyle; **ol**, olecranon. Scale bars equal 5 mm.

(Fig. 7G, H). It is very similar in length and size to the radius, although the latter's shaft appears thicker. The ends are expanded, especially the proximal one, where the olecranon is wide but flattened dorsoventrally; a portion of the proximal head of the bone, including the olecranon, may have been cartilaginous in life, altering the morphology (Romer, 1956).

Manus—Skeletal material can be seen in the carpal region, although it is not articulated, and it is therefore difficult to assign a name to each bone. The biggest bone is interpreted as the ulnare, possibly fused with the pisiform. The number of bones in the wrist area suggests the presence of an intermedium and at least two central bones; the phalanges are elongated,

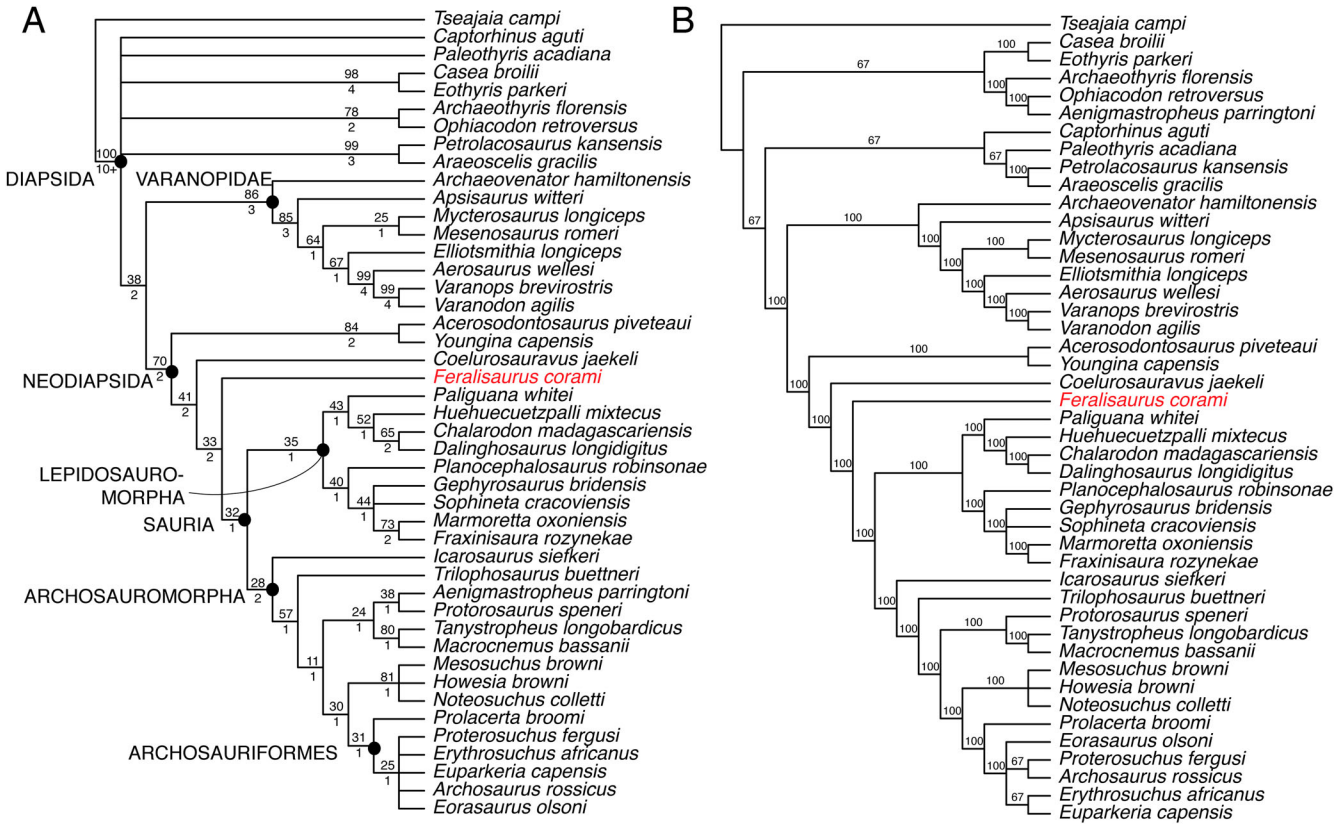

FIGURE 8. Results of phylogenetic analysis that include *Feralisaurus corami* (in red) in the Schoch and Sues (2018) data matrix. **A**, strict consensus tree from parsimony analysis, showing bootstrap and Bremer support values, above and below the line respectively, calculated in the TNT analysis. Tree parameters in PAUP are: tree length (TL) = 883; consistency index (CI) = 0.3296; homoplasy index (HI) = 0.6704; CI excluding uninformative characters = 0.3250; HI excluding uninformative characters = 0.6750; retention index (RI) = 0.6337; rescaled consistency index (RC) = 0.2088. In the TNT parsimony and new technology analyses, this is both the strict and majority rule consensus tree, with TL = 883, CI = 0.315, RI = 0.609. **B**, majority-rule consensus tree from PAUP search, showing tree numbers above the line. 101 trees retained; TL = 883; CI = 0.166; RI = 0.095.

hinting at long digits, and a bone interpreted as an ungual is gently curved and laterally flattened.

PHYLOGENETIC ANALYSES

Feralisaurus is not complete, so the character coding lacks some important cranial characters; nonetheless, phylogenetic analyses were informative. Resolving dubious placements of all the coded taxa is outside the scope of this work, and we focus here on resolving the phylogenetic position and relationships of *Feralisaurus*.

The first analysis used the Schoch and Sues (2018) matrix, which is a modified version of the matrix from Ezcurra et al. (2014). This yielded a best tree score of 879 using PAUP, in line with the results achieved by previous analyses considering the addition of another incomplete taxon, and retaining 108 most parsimonious trees, after exclusion of six uninformative characters (63, 127, 135, 190, 194, 219); tree length is 883 retaining these. We identified two consensus tree topologies: one (Fig. 8A) was the strict consensus tree recovered by the PAUP analysis as well as the strict and majority rule consensus trees from both the TNT parsimony and TNT new technology searches; the other (Fig. 8B) was the majority rule consensus tree recovered from the PAUP analysis.

In both trees, Diapsida, Neodiapsida, Sauria, Archosauromorpha, and Archosauriformes are identified as clades, but with low support values (Fig. 8A). Diapsida includes some unresolved basal taxa, and Neodiapsida includes Younginiformes, *Feralisaurus*, Lepidosauromorpha, and Archosauromorpha as distinct clades. *Feralisaurus* plots within Neodiapsida, as immediate outgroup to Sauria (the clade comprising Archosauromorpha and Lepidosauromorpha), but with low support values. In order to try to improve resolution, basal taxa were eliminated from the analysis, but the results were equally poor. A further step was taken in deleting non-informative characters, while the remaining ones were re-weighted based upon their consistency index (Farris, 1969). The resulting majority rule consensus tree represented no real improvement for overall clade relationships but retrieved *Feralisaurus* in a basal position inside Lepidosauromorpha.

Resolution of the analysis of the Jones et al. (2013) matrix was only slightly better, with a best tree score of 189 and 2,880 trees retained (from both heuristic and branch-and-bound searches). This followed exclusion of 21 uninformative characters (3, 11, 13, 16, 24, 25, 28, 31, 36, 41, 44, 49, 51, 52, 55, 59, 66, 70, 73, 77, and 97). The resulting consensus trees from parsimony (Fig. 9) are very similar to those obtained by Jones et al. (2013). In the 50% majority-rule consensus tree (Fig. 9B), *Youngina* is retrieved as sister taxon of all other neodiapsids, and this comprises an unresolved basal grouping including *Feralisaurus* together with *Saurosternon*, *Paliguana*, Kuehneosauridae, Archosauromorpha (*Czatkowiella* + *Prolacerta*) and Lepidosauromorpha. There is clear support for the clades Lepidosauria and Rhynchocephalia, but poor resolution among Rhynchocephalia, except for a

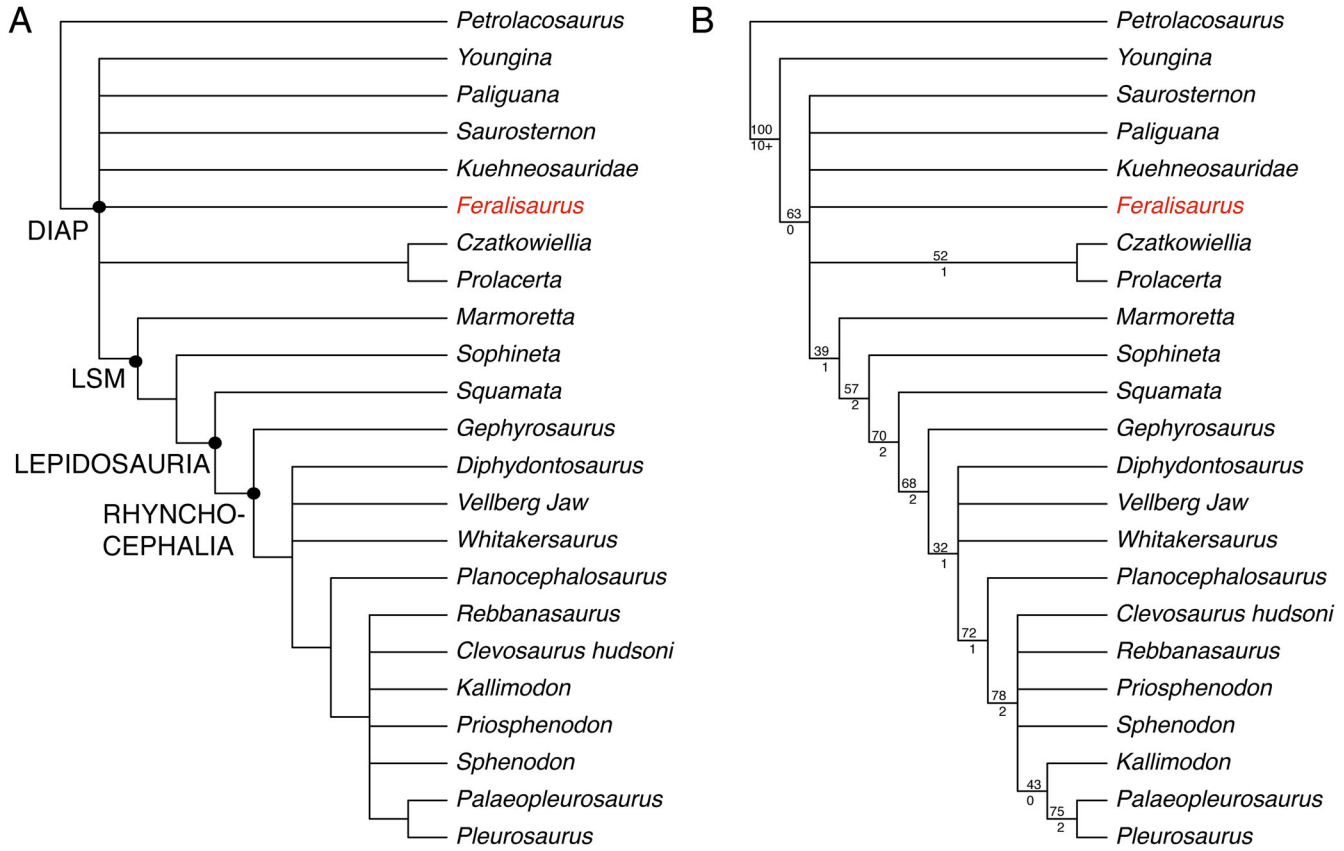

FIGURE 9. Results of phylogenetic analysis that include *Feralisaurus corami* (in red) in the Jones et al. (2013) data matrix. **A**, strict consensus tree from parsimony analysis in PAUP and TNT, and **B**, majority-rule consensus tree, from parsimony analysis in TNT, showing bootstrap and Bremer support values, above and below the line respectively. Tree parameters in PAUP are: tree length (TL) = 189; consistency index (CI) = 0.5556; homoplasy index (HI) = 0.4444; retention index (RI) = 0.7237; rescaled consistency index (RC) = 0.4020. In TNT, TL = 209 (uninformative characters not excluded), CI = 0.553, RI = 0.668. **Abbreviations**: **DIAP**, Diapsida; **LSM**, Lepidosauromorpha.

grouping of *Kallimodon*, *Palaeopleurosaurus*, and *Pleurosaurus* as a clade.

The analyses using the larger data matrices from Scheyer et al. (2020) and Sobral et al. (2020) did not clarify the position of *Feralisaurus*, as it fell in unresolved groupings at the base of Diapsida in both cases. The low support for the most parsimonious trees in all the cladistic analyses and the largely unresolved tree topologies reflect the incompleteness of the fossil record of Triassic archosauromorphs and lepidosauromorphs: roughly one-third of the Schoch and Sues (2018) data matrix used here comprises missing or unknown data, and more than one-third of missing data is concentrated in Lepidosauromorpha. The Jones et al. (2013) matrix is the same, with around 40% of missing data. Adding one incompletely coded taxon to the matrices resulted in augmented general uncertainty, but on the other hand allowed us to place *Feralisaurus* with certainty inside Neodiapsida (as the conservative hypothesis) and possibly within Lepidosauromorpha. The fact that *Feralisaurus* is always recovered as distinct from other coeval taxa suggests it is a distinct taxon. These two issues, whether *Feralisaurus* is a lepidosauromorph and whether it is a distinct new taxon, require further discussion.

DISCUSSION

Feralisaurus as a Lepidosauromorph

Although well preserved in places, the *Feralisaurus* holotype (BRSUG 29950-12) lacks a series of important characters from the skull area, making it difficult to classify. This problem is worsened by the general rarity and incompleteness of similar specimens from the Triassic, making comparisons tricky (Carroll, 1975; Evans, 1991; Waldman and Evans, 1994; Modesto and Reisz, 2003; Evans and Borsuk-Białynicka, 2009; Renesto and Bernardi, 2014; Schoch and Sues, 2018; Simões et al., 2018; Scheyer et al., 2020; Sobral et al., 2020).

In all cladistic analyses (Figs. 8, 9), *Feralisaurus* is identified as a neodiapsid based on the well-developed retroarticular process of the mandible, a notch in the quadrate, and an olecranon only slightly expanded, all of which were identified by Benton (1985) as diagnostic of the clade when he named it. Two further neodiapsid characters, absence of caniniform teeth and reduced lacrimal, are hinted at by the specimen—indeed its teeth are homodont, and no caniniform teeth are identified. Further, three characters of the maxilla of *Feralisaurus* suggest a reduced lacrimal: characters 13, state 1 (presence of a dorsal process of the maxilla), 14, state 1 (the maxilla contacts the prefrontal), and 23, state 1 (lacrimal not involved in the external nares) from the Schoch and Sues (2018) matrix. The preserved materials unfortunately do not allow identification of the diapsid double temporal fenestrae.

Feralisaurus shows a number of apomorphic characters of Lepidosauromorpha, but not all. Its lepidosauromorph characters are (listing character states from Schoch and Sues, 2018, as SS): (1) the shape of the quadrate, which presents a conch and is bowed in lateral view (Gauthier et al., 1988; Evans and Borsuk-Białynicka, 2009; SS character 54, state 2); (2) a small mandibular symphysis made only from the dentary, probably a plesiomorphic condition

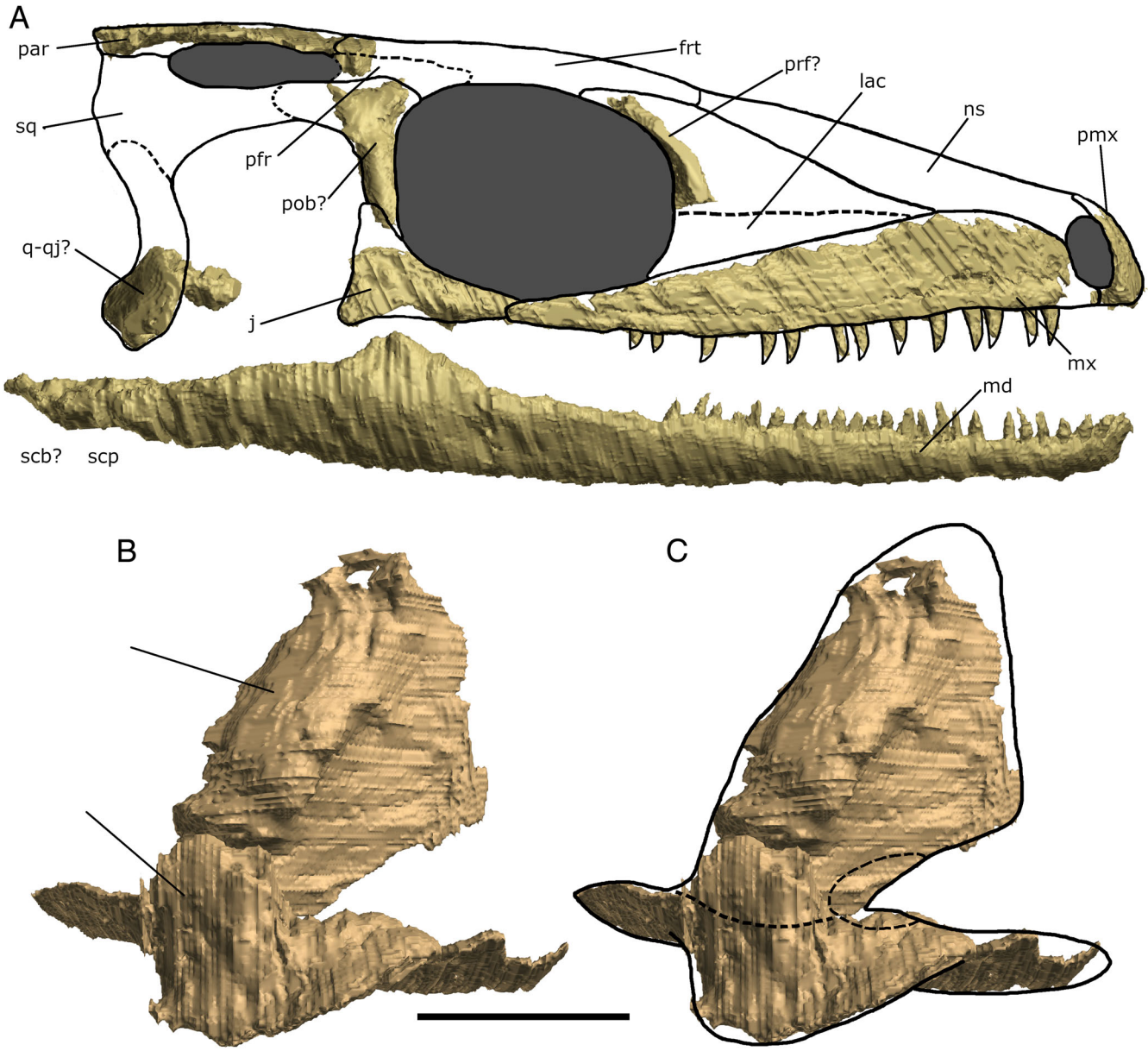

FIGURE 10. *Feralisaurus corami*, gen. et sp. nov. **A**, reconstruction of *Feralisaurus* skull. Solid elements are based on the 3D model, line drawings highlight the missing bones, the skull openings are indicated in dark gray. **B**, **C**, reconstruction of the left scapulocoracoid in left lateral view, **B**, 3D model based and **C**, with a line drawing showing the hypothesized bone morphology in life. **Abbreviations**: **frt**, frontal; **j**, jugal; **lcm**, lacrimal; **md**, mandible; **mx**, maxilla; **ns**, nasal; **par**, parietal; **pfr**, postfrontal; **pmx**, premaxilla; **pob?**, postorbital; **prf?**, prefrontal; **q-qj?**, quadrate; **scb?**, scapular blade; **scp**, scapulocoracoid; **sq**, squamosal. Scale bar equals 5 mm.

for Lepidosauromorpha, shared by taxa such as *Sophineta* and the kuehneosaurids (Evans and Borsuk-Białynicka, 2009); (3) presence of a coronoid process (SS character 158, states 2 and 3); (4) pleurodont dentition (Romer, 1956; Benton, 1985; SS, character 1, state 2); (5) single-headed dorsal ribs (Benton, 1985; SS, character 48, state 1); (6) interclavicle not webbed between lateral and posterior processes (SS, character 82, state 1).

Other characters cannot be confidently determined but are suggested indirectly. The jugal presents a modest posteriorly directed process, and thus an incomplete lower temporal bar might be assumed. In the same way, the jugal and maxilla complex suggests that the maxilla's suborbital process enters the orbit (Evans and Borsuk-Białynicka, 2009), all characters of Lepidosauromorpha.

Feralisaurus lacks some diagnostic lepidosauromorph characters: absence of capitulum and trochlea (SS, character 198, state 2), whereas the humerus of *Feralisaurus* presents these features weakly but distinctly; the ectepicondylar region (SS, character 91) is bridged and presents a foramen for Lepidosauromorpha, but has no processes or grooves in *Feralisaurus* (states 0 and 2, respectively); the lepidosauromorph-like prominent olecranon (SS, character 94, state 1) is reduced in *Feralisaurus.*

There is no evidence to suggest that *Feralisaurus* might be associated with any particular clade within Lepidosauromorpha. The presence of splenials and the pleurodont dentition exclude *Feralisaurus* from Sphenodontia, because even in the most basal members of Sphenodontia splenials are absent and tooth implantation is generally acrodont (Benton, 1985; Jones et al., 2013).

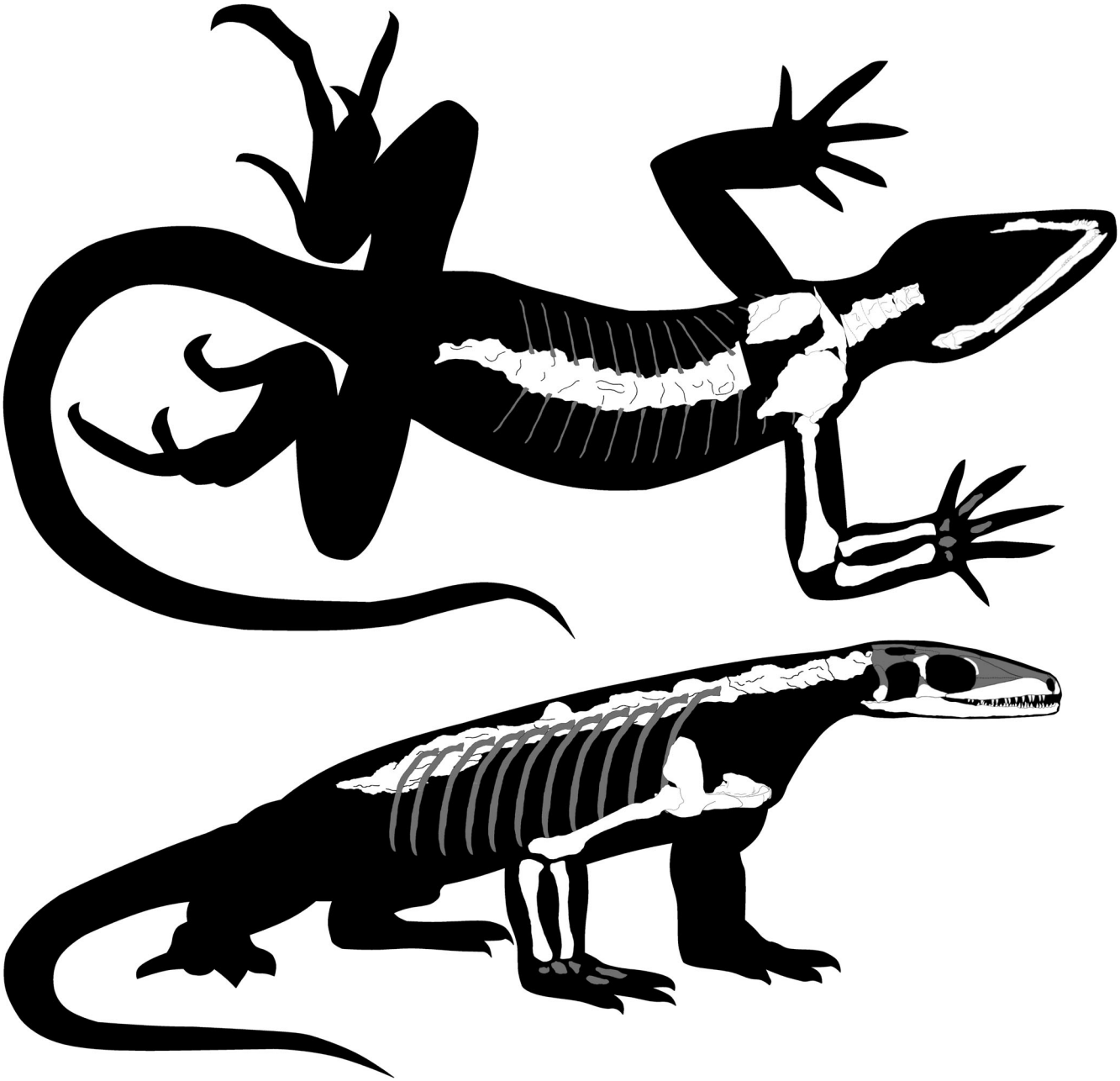

FIGURE 11. Skeletal restoration of *Feralisaurus* in **A**, dorsal and **B**, lateral views. Wherever possible, bones are drawn based on the 3D model in an appropriate perspective (white). Bones in gray are reconstructed or of dubious interpretation. In **A**, part of the ribcage and vertebral column is obscured to allow a better view of the pectoral girdle. The black silhouettes are based entirely upon extant reptiles.

Further, no characters support an affinity of *Feralisaurus* to clades like Kuehneosauridae or Younginiformes (Benton, 1985; Evans, 2009; Jones et al., 2013) as it lacks the specialized post-cranial adaptations of gliders and has an incomplete lower temporal bar. In the Jones et al. (2013) analysis, *Feralisaurus* shares three apomorphies with the clade *Marmoretta* + *Sophineta* + Squamata: presence of splenials (char. 35, 1), pleurodont anterior dentition (char. 40, 1), single headed ribs (char. 48, 1).

As a further test of affinities, a search was made for any archosauromorph characters. The only detectable archosauromorph-like character of *Feralisaurus* is the presence of a weak capitulum and trochlea on the distal end of the humerus (SS, character 198, state 1). The specimen lacks a lateral mandibular fenestra, tooth serration and thecodont tooth implantation, cervical vertebrae similar in length to anterior dorsals, an acromion process and a posteroventral tuber on the scapulocoracoid (Nesbitt, 2011). The antorbital fenestra, an important synapomorphy of Archosauriformes, is absent.

The cladistic analyses show that *Feralisaurus* is a neodiapsid, and basal to the two major clades that comprise Sauria, namely Lepidosauromorpha and Archosauromorpha. We argue that *Feralisaurus* is almost certainly a lepidosauromorph, based on possession of six apomorphies, and absence of all detectable archosauromorph apomorphies. This was not identified in the cladistic analyses as *Feralisaurus* and critical comparator taxa from the Triassic are incompletely coded and the consensus trees (Fig. 8,

9) provide a conservative view. Furthermore, the specimen age (Anisian) is coherent with existing literature about the estimated divergence times between Archosauromorpha and Lepidosauromorpha (Benton and Donoghue, 2007; Donoghue and Benton, 2007; Jones et al., 2013; Ezcurra et al., 2014; Simões et al., 2018).

Feralisaurus as a New Taxon

Feralisaurus is incomplete, but it was possible to retrieve enough evidence to diagnose it as a new genus and species, distinguishing it from other Triassic diapsids. The ventrolateral process of both scapulocoracoids seems to be a rather peculiar character of *Feralisaurus*, at least among those members of Lepidosauromorpha for which the pectoral girdle is known. We now consider each genus to which we could have reasonably assigned *Feralisaurus*, and the differences.

The first comparisons were carried out with the Otter Sandstone biota, including procolophonids, a few archosaur groups, and rare lepidosauromorphs (Spencer and Isaac, 1983; Milner et al., 1990; Benton, 1997; Spencer and Storrs, 2002; Benton, 2011; Coram and Radley, 2015; Coram et al., 2019; Zaher et al., 2019). The only small diapsid, *Coartaredens* (Spencer and Storrs, 2002), can easily be distinguished from *Feralisaurus* in its tooth and mandible morphology, and the number of teeth on the dentary.

Some Triassic clades show enough specialization to be an impossible match for *Feralisaurus*, such as Drepanosauridae (Pinna, 1986; Berman and Reisz, 1992) and Kuehneosauridae (Evans, 1988, 2009), and they were discarded with confidence.

Among coeval Lepidosauromorpha, *Megachirella* from the Middle Triassic of northern Italy (Renesto and Posenato, 2003; Simões et al., 2018) has a lower coronoid process, a longer and pointed posterior jugal process, non-notochordal vertebrae, a less expanded humerus proximal end and a completely open entepicondylar foramen. *Fraxinisaura* from the Middle Triassic of Germany (Schoch and Sues, 2018) possesses a very different maxilla, generally low but with an evident facial process, markedly recurved teeth, a different dentary morphology, non-notochordal vertebrae, a cruciform interclavicle and a complete entepicondylar foramen. Finally, *Sophineta* from the Early Triassic of Poland (Evans and Borsuk-Białynicka, 2009) has a very high maxillary facial process, a smaller posterior process on the jugal (even in the larger retrieved jugals), compressed tooth tips and no transverse processes on the vertebrae.

Although stratigraphically much younger, *Marmoretta* from the Middle Jurassic of England and Scotland (Evans, 1991; Waldman and Evans, 1994) is often identified as a stem lepidosauromorph; the strongest difference lies in this taxon's low maxilla, with a weak facial process.

Four Permian to Early Triassic taxa can also be considered. *Lanthanolania* from the middle Permian of Russia (Modesto and Reisz, 2003) has a very slender and elongated maxillary suborbital ramus that does not enter the ventral side of the orbit, an elongated jugal, an interpreted 30 tooth positions and a 'splint-like' coronoid process, very unlike the stout process of *Feralisaurus*. *Saurosternon* from the Upper Permian or Lower Triassic of South Africa (Huxley, 1868; Carroll, 1975) differs from *Feralisaurus* in having no ventral keels on the vertebral centra, a markedly different morphology of the scapulocoracoid (especially posteriorly), different epipodial-propodial proportions (Carroll, 1975) and a smaller and stouter humerus compared with the rest of the skeleton. *Palaeagama* from the Late Permian of South Africa (Carroll, 1975) differs from *Feralisaurus* in its jugal morphology, with no posterior process and an elongated anterior process which excludes the maxilla from the orbit; the maxilla in turn is smaller and low, the dentition is sub-pleurodont, and the humerus shaft is expanded near each end, especially the distal end. Finally, *Paliguana* from the Lower Triassic of South Africa (Carroll, 1975; Evans and Jones, 2010) differs from *Feralisaurus* in the maxilla (incomplete in the specimen) which is interpreted as low and not involved in the ventral side of the orbit, and a jugal with a long anterior process.

Considering all the above, *Feralisaurus* is a new genus of lepidosauromorph reptile; its relationships among Lepidosauromorpha are unclear, since its morphology shows a mix of primitive and derived characters.

Skeletal Reconstruction

A full skeletal reconstruction of *Feralisaurus* cannot be attempted in the absence of data; the lack of articulated hind limbs, sacral girdle and tail seems to be a common taphonomic feature shared with other Triassic lepidosauromorphs (Renesto and Posenato, 2003; Evans and Borsuk-Białynicka, 2009; Schoch and Sues, 2018), making it difficult to base a reconstruction on another taxon. Two interesting areas for which a reconstruction was attempted are the scapulocoracoid and the skull.

The skull is badly damaged, so its reconstruction (Fig. 10A) should be considered more tentative than that of the scapulocoracoid, but in turn there are many Triassic lepidosauromorph skulls to base a reconstruction upon. The skull's height is approximated from the jugal, the postorbital and the curvature of the premaxillae; for many other elements, size and shape are based upon *Fraxinisaura* and *Sophineta* (Evans and Borsuk-Białynicka, 2009; Schoch and Sues, 2018). Given the primitive morphology of the maxilla, the presence of a lacrimal can be inferred, but its involvement in the orbit is dubious, and the snout was probably intermediate between the high and bulky *Sophineta* snout and the longer, more slender one of *Fraxinisaura*.

The left scapulocoracoid was chosen for reconstruction, although it is incomplete, because of the notable bone fragment that lies next to it, visible on the specimen's surface (Figs. 2, 3). We tested the hypothesis that the fragment is the scapula blade, deformed and broken off from the rest of the scapulocoracoid, through a 3D reconstruction (Fig. 10B, C). The fragment is incompatible with other possible interpretations, such as the proximal head of the left humerus or the posterior-most portion of the coracoid, because of its morphology. The best fit was to put it on top of the scapulocoracoid: allowing room for deformation, the scapula blade is higher than wide, slightly flared dorsoposteriorly and presents a supraglenoid buttress. This reconstruction sadly does not provide more details about the glenoid area, damaged in both scapulocoracoids.

Both reconstructions were subsequently incorporated and rearranged in life position, along with all other identifiable skeletal material (Fig. 11A, B). The starting silhouettes are modeled after existing lacertids and iguanids and have been modified to fit the specimen's dimensions, while the bones are taken from the 3D model without modification other than in their positions or perspective; this allows us to approximate what *Feralisaurus* may have looked like and to accommodate the bones in life positions.

Ontogeny and Inferences on Mode of Life

The bones in specimen BRSUG 29950-12 clearly belong to a single *Feralisaurus* individual. The ends of the forelimb bones were difficult to segment for the 3D model, but there is no evidence that they were cartilaginous. No suture was found between scapulae and coracoids so, although the teeth are too small to find details of wear at the scan resolution, the specimen's ontogenetic status is probably beyond juvenile.

Feralisaurus is one of the smallest terrestrial vertebrates discovered so far in the Otter Sandstone biota, with an estimated presacral length of 120–132 mm; its weight compared to extant Squamata of similar morphology, like the genus *Lacerta*, could have been 30–50 g (Meiri, 2010). There are no signs of adaptations to aquatic or arboreal lifestyles in its morphology; in addition, the relatively long humerus (roughly equal to six dorsal centra) suggests *Feralisaurus* was a land-dwelling animal.

The dentition strongly suggests a predatory mode of life, but the animal's dimensions and morphology make it unlikely that it would have preyed on other known vertebrates from the Otter Sandstone. It is likely that *Feralisaurus* was principally insectivorous, feeding on terrestrial arthropods or perhaps in an opportunistic way on smaller undiscovered vertebrates that inhabited the forested proximities of the ancient river. It is likely that it was preyed upon by larger carnivorous vertebrates, such as the rauisuchians and temnospondyl amphibians (Coram et al., 2019).

ACKNOWLEDGMENTS

We thank R. A. Coram for finding this specimen and for his commitment to having his fossils described, T. G. Davies for scanning the specimen and for his assistance with software and technical issues, the University of Bristol for accepting I.C. as a visiting post-graduate student and J. Pignatti from Università di Roma 'La Sapienza' for co-supervising I.C.'s final M.Sc. project. We thank R.A. Coram also for Figure 1. I.C.'s visit to the University of Bristol was possible thanks to a Università di Roma 'La Sapienza' grant for M.Sc. theses abroad (n. 9/2018). Additional funding came from a University of Bristol Ph.D. grant to M.Z., and NERC grant NE/P013724/1 to M.J.B.

ORCID

Michael J. Benton http://orcid.org/0000-0002-4323-1824

LITERATURE CITED

Abel, R. L., C. Laurini, and M. Richter. 2012. A palaeobiologist's guide to 'virtual' micro-CT preparation. Palaeontologica Electronica 15. palaeo-electronica.org/content/issue-2-2012-technical-articles/233-micro-ct-workflow

Ambrose, K., E. Hough, N. J. P. Smith, and G. Warrington. 2014. Lithostratigraphy of the Sherwood Sandstone Group of England, Wales and south-west Scotland. British Geological Survey Research Report RR/14/01:1–50.

Benton, M. J. 1985. Classification and phylogeny of the diapsid reptiles. Zoological Journal of the Linnean Society 84:97–164.

Benton, M. J. 1997. The Triassic reptiles from Devon. Proceedings of the Ussher Society 9:141–152.

Benton, M. J. 2011. Archosaur remains from the Otter Sandstone Formation (Middle Triassic, late Anisian) of Devon, southern UK. Proceedings of the Geologists' Association 122:25–33.

Benton, M. J., and Donoghue, P. C. J. 2007. Palaeontological evidence to date the tree of life. Molecular Biology and Evolution 24:26–53.

Berman, D. S., and R. R. Reisz. 1992. *Dolabrosaurus aquatilis*, a small lepidosauromorph reptile from the Upper Triassic Chinle Formation of north-central New Mexico. Journal of Paleontology 66:1001–1009.

Carroll, R. L. 1975. Permo-Triassic "lizards" from the Karroo. Palaeontologia Africana 18:71–87.

Coram, R. A., and J. D. Radley. 2015. Chirothere footprint sites from the Otter Sandstone Formation (Middle Triassic, late Anisian) of Devon, United Kingdom. Ichnos 22:29–42.

Coram, R. A., J. D. Radley, and M. J. Benton. 2019. The Middle Triassic (Anisian) Otter Sandstone biota (Devon, UK): Review, recent discoveries and ways ahead. Proceedings of the Geologists' Association 130:294–306.

Donoghue, P. C. J., and Benton, M. J. 2007. Rocks and clocks: calibrating the Tree of Life using fossils and molecules. Trends in Ecology and Evolution 22:424–431.

Evans, S. E. 1988. Crown group lizards (Reptilia, Squamata) from the Middle Jurassic of the British Isles. Palaeontographica Abteilung A 250:123–154.

Evans, S. E. 1991. A new lizard-like reptile (Diapsida: Lepidosauromorpha) from the Middle Jurassic of England. Zoological Journal of the Linnean Society 103:391–412.

Evans, S.E. 2003. At the feet of the dinosaurs: the early history and radiation of lizards. Biological Reviews 78:513–551.

Evans, S. E. 2009. An early kuehneosaurid reptile from the Early Triassic of Poland. Palaeontologia Polonica 65:145–178.

Evans, S. E., and M. Borsuk-Białynicka. 2009. A small lepidosauromorph reptile from the early Triassic of Poland. Palaeontologia Polonica 65:179–202.

Evans, S. E., and M. E. H. Jones. 2010. The origin, early history and diversification of lepidosauromorph reptiles; pp. 27–44 in S. Bandyopadhyay (ed.), New Aspects of Mesozoic Biodiversity. Springer, Berlin.

Evans, S. E., G. V. R. Prasad, and B. K. Manhas. 2002. Fossil lizards from the Jurassic Kota Formation of India. Journal of Vertebrate Paleontology 22:299–312.

Ezcurra, M. D., T. M. Scheyer, and R. J. Butler. 2014. The origin and early evolution of Sauria: reassessing the Permian saurian fossil record and the timing of the crocodile-lizard divergence. PLoS ONE 9:e89165.

Farris, J. S. 1969. A successive approximations approach to character weighting. Systematic Zoology 18:374–385.

Gallois, R. W. 2013. Possible tetrapod burrows in the Mid Triassic Otter Sandstone Formation at Sidmouth, Devon, UK. Geoscience in South-West England 13:208–215.

Gauthier, J. A. 1984. A cladistic analysis of the higher systematic categories of the Diapsida. Ph.D. dissertation, University of California, Berkeley.

Gauthier, J., A. G. Kluge, and T. Rowe. 1988. Amniote phylogeny and the importance of fossils. Cladistics 4:105–208.

Goloboff, P. A., J. S. Farris, and K. C. Nixon. 2008. TNT, a free program for phylogenetic analysis. Cladistics 24:774–786.

Gow, C. E. 1975. The morphology and relationships of *Youngina capensis* Broom and *Prolacerta broomi* Parrington. Palaeontologica Africana 18:89–131.

Hounslow, M. W., and McIntosh, G. 2003. Magnetostratigraphy of the Sherwood Sandstone Group (Lower and Middle Triassic) south Devon, UK; detailed correlation of the marine and non-marine Anisian. Palaeogeography, Palaeoclimatology, Palaeoecology 193:325–348.

Huxley, T. H. 1868. On *Saurosternon bainii*, and *Pristerodon mckayi*, two new fossil lacertilian reptiles from South Africa. Geological Magazine 47:201–205.

Jones, M. E. H., C. L. Anderson, C. A. Hipsley, J. Müller, S. E. Evans, and R. R. Schoch. 2013. Integration of molecules and new fossils supports a Triassic origin for Lepidosauria (lizards, snakes, and tuatara). BMC Evolutionary Biology 13:208.

Meiri, S. 2010. Length-weight allometries in lizards. Journal of Zoology 281:218–226.

Milner, A. R., B. G. Gardiner, N. C. Fraser, and M. A. Taylor. 1990. Vertebrates from the Middle Triassic Otter Sandstone Formation of Devon. Palaeontology 33:873–892.

Modesto, S. P., and R. R. Reisz. 2003. An enigmatic new diapsid reptile from the Upper Permian of Eastern Europe. Journal of Vertebrate Paleontology 22:851–855.

Nesbitt, S. J. 2011. The early evolution of archosaurs: relationships and the origin of major clades. Bulletin of the American Museum of Natural History 352:1–292.

Newell, A. J. 2018. Rifts, rivers and climate recovery: A new model for the Triassic of England. Proceedings of the Geologists' Association 129:352–371.

Osborn, H. F. 1903. The reptilian subclasses Diapsida and Synapsida and the early history of the Diaptosauria. Memoirs of the American Museum of Natural History 1:449–507.

Pinna, G. 1986. On *Drepanosaurus unguicaudatus*, an Upper Triassic lepidosaurian from the Italian Alps. Journal of Paleontology 60:1127–1132.

Renesto, S., and M. Bernardi. 2014. Redescription and phylogenetic relationships of *Megachirella wachtleri* Renesto et Posenato, 2003 (Reptilia, Diapsida). Paläontologische Zeitschrift 88:197–210.

Renesto, S., and R. Posenato. 2003. A new lepidosauromorph reptile from the Middle Triassic of the dolomites (Northern Italy). Rivista Italiana di Paleontologia e Stratigrafia 109:463–474.
Romer, A. S. 1956. Osteology of Reptiles. University of Chicago Press, Chicago, 772 pp.
Scheyer, T. M., S. N. F. Spiekman, H.-D. Sues, M. D. Ezcurra, R. J. Butler, and M. E. H. Jones. 2020. *Colobops*: a juvenile rhynchocephalian reptile (Lepidosauromorpha), not a diminutive archosauromorph with an unusually strong bite. Royal Society Open Science 7 (3):192179.
Schoch, R. R., and H.-D. Sues. 2018. A new lepidosauromorph reptile from the Middle Triassic (Ladinian) of Germany and its phylogenetic relationships. Journal of Vertebrate Paleontology 38: e1444619.
Simões, T. R., Vernygora, O., Caldwell, M. W., and Pierce, S. E. 2020. Megaevolutionary dynamics and the timing of evolutionary innovation in reptiles. Nature Communications 11:3322.
Simões, T. R., M. W. Caldwell, M. Tałanda, M. Bernardi, A. Palci, O. Vernygora, F. Bernardini, L. Mancini, and R. L. Nydam. 2018. The origin of squamates revealed by a Middle Triassic lizard from the Italian Alps. Nature 557:706–709.
Sobral, G., T. R. Simões, and R. R. Schoch. 2020. A tiny new Middle Triassic stem-lepidosauromorph from Germany: implications for the early evolution of lepidosauromorphs and the Vellberg fauna. Scientific Reports 10(1):e2273
Spencer, P. S., and K. P. Isaac. 1983. Triassic vertebrates from the Otter Sandstone Formation of Devon, England. Proceedings of the Geologists' Association 94:267–269.
Spencer, P. S., and G. W. Storrs. 2002. A re-evaluation of small tetrapods from the Middle Triassic Otter Sandstone Formation of Devon, England. Palaeontology 45:447–467.
Swofford, D. L. 2015. PAUP*. Phylogenetic Analysis Using Parsimony (*and Other Methods), version 4.0. Sinauer Associates, Sunderland, Massachusetts.
Waldman, M., and S. E. Evans. 1994. Lepidosauromorph reptiles from the Middle Jurassic of Skye. Zoological Journal of the Linnean Society 112:135–150.
Zaher, M., R. A. Coram, and M. J. Benton. 2019. The Middle Triassic procolophonid *Kapes bentoni*: computed tomography of the skull and skeleton. Papers in Palaeontology 5:111–138.

Submitted June 29, 2019; revisions received April 23, 2020;
accepted May 5, 2020.
Handling Editor: Jason Head.

APPENDIX

Feralisaurus corami Coded for the Jones et al. (2013) Data Matrix

Feralisaurus corami
?????????3??????1????????1???1????1??0?2?????011???
00?????????????????????????0??0?????000??0??200?2000

Feralisaurus corami Coded for the Schoch and Sues (2018) Data Matrix

Feralisaurus corami
2100?{12}???? ??{01}?00-??? ?????????? ???????{12}{12}{34}
?????????? ????2?????1 ?1????00?? ??20???1?? 100???011?
2010?????? ?????????? ????0??0?? 111?00???? ??????????
?????????? ???????{23}00 ?????00??? ???0?????? ????0?????
????000110 01???????? ?????????0 ?